New Culvert Projections for Washington State:

Improved Modeling, Probabilistic Projections, and an Updated Web Tool

GUILLAUME MAUGER | UW CIG
MINGLIANG LIU | WSU
JENNY ADAM | WSU
JASON WON | UW CIG
GEORGE WILHERE | WDFW
DAN DULAN | WDFW
JANE ATHA | WDFW
LYNN HELBRECHT | WDFW
TIM QUINN | WDFW

SEPTEMBER 2021

CLIMATE IMPACTS GROUP

COVER PAGE PHOTO CREDIT: Culvert by Tom Gill, used CC BY-NC-ND 2.0

ACKNOWLEDGEMENTS:

This work was supported by USGS Northwest Climate Adaptation Science Center. Additional support was provided by the Washington State Department of Natural Resources. Regional climate model simulations were provided by Ruby Leung at Pacific Northwest National Laboratory and Cliff Mass in the UW Department of Atmospheric Sciences.

CITATION:

Mauger, G.S., M. Liu, J.C. Adam, J. Won, G. Wilhere, D. Dulan, J. Atha, L. Helbrecht, and T. Quinn (2021). *New Culvert Projections for Washington State: Improved Modeling, Probabilistic Projections, and an Updated Web Tool*. Report prepared for the Northwest Climate Adaptation Science Center. Climate Impacts Group, University of Washington.

GRANT INFORMATION (NW CASC):

Recipient	Guillaume Mauger
Agency/Institution	University of Washington Climate Impacts Group
Project Title	Supporting Climate-Resilient Design for In-Stream Restoration and Fish Passage Projects
Agreement Number	G19AC00005
Date of Report	Sunday, July 3, 2022
Period of Time Covered by the Report	December 2018 – December 2021
Total Award	$149,633.98

TABLE OF CONTENTS

Introduction and Background

Climate change is projected to significantly alter streamflow in much of the Pacific Northwest. Building on previous work, the purpose of this study is to develop new up-to-date site-level projections of changes in streamflow and channel width for use in climate-resilient culvert and instream restoration design.

Washington State's Culvert Design Standard

Apart from a few special cases, culverts in Washington State are required to follow the stream simulation design (WAC 220-660-190(6)) which was developed by the Washington Department of Fish and Wildlife in the 1990s (WDFW; Cenderelli et al. 2011). The stream simulation design is based on geomorphic principles, which lead to an inference that the most important geomorphic parameter in culvert design is channel width. Hence, the stream simulation design specifies culvert width as a function of channel width (Barnard et al. 2013):

$$Culvert\ Width = 1.2 \times BFW + 2\ ft \qquad \text{Eq. 1}$$

where culvert width is measured at the streambed and BFW is bankfull width of the stream channel measured in feet. Bankfull width is a well-established parameter that is generally straightforward to estimate in the field, though in some instances it can be obscured by debris flows, vegetation loss, anthropogenic disturbances, or the presence of multiple channels.

Previous Work

Wilhere et al. (2016) estimated future changes in BFW using hydrologic projections developed by Hamlet et al. (2013), providing estimates of the percent change in BFW. This percent change can then be applied to direct observations of current channel width for the purpose of designing climate-adapted culverts. This approach reduces the influence of bias in the hydrologic simulations. Wilhere et al. suggest using two metrics for evaluating changes in BFW: (1) percent change in BFW, and (2) number of models projecting an increase in BFW. As an example, they propose defining "actionable" locations as those for which the mean increase in BFW is >5% and for which at least 6 of the 10 models show an increase.

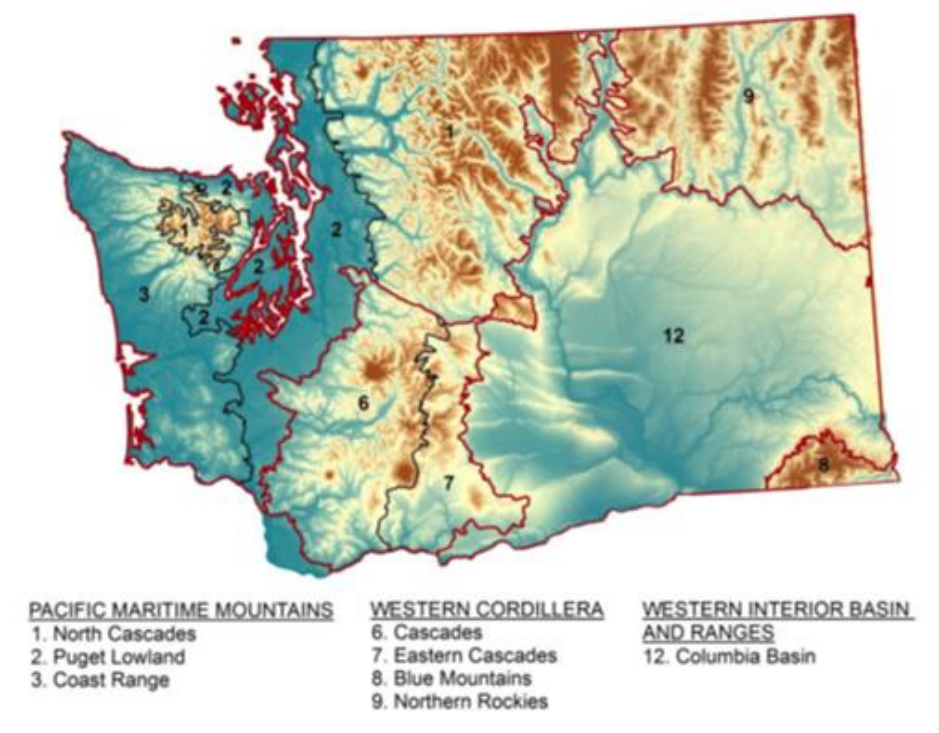

Figure 1. Ecoregions used to define the parameters relating bankfull width (BFW) to peak streamflow statistics across Washington State (Castro and Jackson 2001). *Source:* Copied, with permission, from Wilhere et al. 2016.

Wilhere et al. (2016) estimated current and future bankfull widths by using the empirically-based regressions developed by Castro and Jackson (2001) for a wide range of streams across the Pacific Northwest. In that study, Castro and Jackson relate BFW and peak streamflow statistics via a power relationship:

$$BFW = \alpha Q^{\beta} \qquad \text{Eq. 2}$$

Where Q is the bankfull discharge and α and β are fitted parameters that relate streamflow to BFW. Different sets of parameters were estimated for three different ecoregions in Washington State: Pacific Maritime Mountains, the Western Cordillera, and the Columbia Plateau (Table 1, Figure 1). In Castro and Jackson (2001), as in our analysis, bankfull discharges were

Table 1. Parameters used to relate bankfull width (BFW) to peak streamflow statistics. The parameter α is included even though it is not used in our analysis. *Source:* Castro and Jackson (2001).

Ecoregion	Q	α	β
Pacific Maritime Mountains	1.2-yr	2.37	0.50
Western Cordillera	1.5-yr	3.50	0.44
Columbia Plateau	1.4-yr	0.96	0.60

estimated from the water year maxima in daily observed flows.

In a subsequent update, Mauger et al. (2018) built on the approach of Wilhere et al. (2016) to prototype a probabilistic evaluation of the implications of climate change for culvert design. To do this, Mauger et al. used a slightly different product that nonetheless stemmed from the same statistically-downscaled hydrologic projections used by Wilhere et al. (2016). In their probabilistic approach, Mauger et al. (2018) developed a unique probability distribution for each future year, using this to estimate the probability that a culvert's width (either proposed or "as built") would be inadequate as a result of climate change at some time over the culvert's expected service life (see also Byun et al. 2020). These new results were incorporated into a prototype tool to facilitate climate-resilient culvert design.

Both previous studies relied on statistically downscaled projections. Global climate models (GCMs) represent the climate at coarse spatial scales, and therefore need to be "downscaled" to estimate the corresponding changes at local scales. There are two general approaches to downscaling: (1) statistical, in which empirical relationships between historical GCM simulations and surface weather observations are extrapolated forward in time, and (2) dynamical, in which a GCM is used to drive a finer-scale regional climate model. Statistical approaches are inexpensive to implement and readily available, but are less reliable in topographically complex areas, especially where few observations are available. Dynamical approaches capture important physical processes that are absent from statistical downscaling (Salathé et al. 2010), but are restricted to only a few GCM projections and have not been as thoroughly tested. For example, although there are a few hydrologic datasets based on dynamically downscaled projections (e.g., Salathé et al. 2010), there are currently none that include a large enough number of GCM projections to estimate a range, or uncertainty, in projections.

The work described in this report builds on these previous studies but differs in four overarching ways:

1. By using dynamically downscaled projections, since these have been shown to better capture changes in heavy rain events,
2. By using a newer version of the hydrologic model, updated with new land cover, and a more tailored approach to calibration.

3. By updating the probabilistic projections to better reflect conventions in the statistics and climate science literature, and
4. By integrating the new projections into the WDFW tool so that users have just one online resource for designing climate-adapted culverts.

Our methods and results are described in the sections that follow.

Potential Management Applications

The primary management application for this work is in the design of fish passage culverts in Washington State. There is currently no regulatory standard requiring that culverts be designed to accommodate future flows. Nonetheless, several Washington jurisdictions, engineering consultants, and other prospective users have expressed an interest in installing climate-adapted culverts. This has been evident in the interest generated by the current tool, based on the results of Wilhere et al. (2016). In addition, it is likely that stormwater and other regulations will increasingly be required or incentivized to include climate change considerations in their planning and project design.

We also anticipate that this work may be used by a variety of state and federal agencies. The Washington State Department of Natural Resources has expressed interest in using these projections to design culverts on lands they manage. Similarly, the National Park Service has recently completed a report identifying issues relating to culverts in North Cascades National Park. Another potential application is Section 7 consultation under the under the Endangered Species Act. In Section 7 consultations, the US Fish and Wildlife Service could use the new projections to either provide suggestions on project design or as a basis for evaluating mitigation proposals.

Methods

Climate Data

This section describes the downscaled climate projections used in the current study, and how they were validated and bias-corrected for use in the hydrologic modeling. As noted above, recent research has emphasized the need to use regional climate model projections (or "dynamical downscaling") in order to better quantify changes in extreme precipitation (e.g., Salathé et al. 2014). In this work we made use of existing regional climate model simulations, all performed using the Weather Research and Forecasting model (WRF, Skamarock et al. 2005).

Observationally-Based Historical Climate Dataset

Past hydrologic studies have typically used interpolated estimates of daily weather on model grid cells (e.g., Hamlet et al., 2013). A novel aspect of the current approach is that we use dynamically downscaled historical meteorology, as is done for the climate change simulations. This has a number of advantages. First, we are able to use hourly meteorology as opposed to daily; a significant improvement given that design standards, and the empirical relationships to channel geometry, are typically based on instantaneous peak flows. Second, regional models have been shown to better represent spatial variations in weather variables, particularly in complex topography or where observations are sparse (e.g., Salathé et al. 2014). Finally, by using the same regional climate model for both the historical and climate change simulations, we ensure that the hydrologic model is better adapted to accurately reflect the implications of climate change for hydrology.

For the historical dataset we used an implementation of WRF developed by Ruby Leung and colleagues at the Pacific Northwest National Laboratory (hereafter referred to as "WRF-OBS"). The dataset is produced using WRF version 3.2, with a model domain covering all of the western U.S., at an hourly time step and a spatial resolution of 6 km (Chen et al., 2018). Boundary conditions are taken from the North American Regional Reanalysis (NARR; Mesinger et al., 2006), and the simulation spans the years 1981-2015. Reanalysis datasets are essentially internally-consistent collections of weather observations; they are created by combining massive amounts of environmental observations in a Bayesian model

Table 2. The twelve global climate models (GCMs) used as input to the regional model simulations. All simulations are based on the high-end RCP 8.5 greenhouse gas scenario (Van Vuuren et al., 2011). A low-end scenario was also produced for the ACCESS 1.0 model, resulting in two separate projections for this GCM.

Model	Center	Resolution (degrees)	Vertical Levels
ACCESS1-0	Commonwealth Scientific and Industrial Research Organization (CSIRO), Australia/ Bureau of Meteorology, Australia	1.25 x 1.88	38
ACCESS1-3	Commonwealth Scientific and Industrial Research Organization (CSIRO), Australia/ Bureau of Meteorology, Australia	1.25 x 1.88	38
bcc-csm1-1	Beijing Climate Center (BCC), China Meteorological Administration	2.8 × 2.8	26
CanESM2	Canadian Centre for Climate Modeling and Analysis	2.8 × 2.8	35
CCSM4	National Center of Atmospheric Research (NCAR), USA	1.25 × 0.94	26
CSIRO-Mk3-6-0	Commonwealth Scientific and Industrial Research Organization (CSIRO) / Queensland Climate Change Centre of Excellence, Australia	1.8 × 1.8	18
FGOALS-g2	LASG, Institute of Atmospheric Physics, Chinese Academy of Sciences	2.8 × 2.8	26
GFDL-CM3	NOAA Geophysical Fluid Dynamics Laboratory, USA	2.5 × 2.0	48
GISS-E2-H	NASA Goddard Institute for Space Studies, USA	2.5 × 2.0	40
MIROC5	Atmosphere and Ocean Research Institute (The University of Tokyo), National Institute for Environmental Studies, and Japan Agency for Marine-Earth Science and Technology	1.4 × 1.4	40
MRI-CGCM3	Meteorological Research Institute, Japan	1.1 × 1.1	48
NorESM1-M	Norwegian Climate Center, Norway	2.5 × 1.9	26

framework that synthesizes them into the best estimate of the atmospheric state for each time step. NARR is produced for North America at a spatial resolution of 32 km.

Future Climate Dataset

A new ensemble of regional climate model projections was recently produced in collaboration with Cliff Mass in UW's department of Atmospheric Sciences (hereafter referred to as "WRF-GCM"). GCM projections were obtained from the Climate Model Inter-comparison Project, phase 5 (CMIP5; Taylor et al., 2012). Twelve GCMs were selected primarily based on Brewer et al. (2016), who evaluated and ranked global climate models based on their ability to reproduce the climate of the Pacific Northwest. The new ensemble of WRF projections includes one simulation for each of the GCMs listed in Table 1. All of the new projections are based on the high-end RCP 8.5 scenario (Van Vuuren et al., 2011), with the exception of the ACCESS 1.0 GCM, for which an additional simulation was also produced for the low-end RCP 4.5 scenario. Simulations were performed using WRF version 3.2 implemented following Salathé et al. (2010, 2014). The innermost domain, at 12-km resolution, encompasses the U.S. Pacific Northwest. Simulations span the years 1970-2099 at an hourly time step and a spatial resolution of 12 km. The model, and model configuration, are described in detail in Lorente-Plazas et al. (2018) and Mauger et al. (2018). Best practice in climate impacts assessment is to consider several greenhouse gas scenarios – for example, results for the low-end RCP 4.5 scenario for comparison with the high-end RCP 8.5 projections. In our case this is not an option – only RCP 8.5 projections have been dynamically downscaled for the region. Mauger et al. (2019) discuss approaches for using RCP 8.5 projections as an analog for what might be projected for the RCP 4.5 scenario. For example, temperature changes for the 2080s in the RCP 4.5 projections appear to correspond approximately to the projections for the 2040s or 2050s in the RCP 8.5 projections.

Evaluating the WRF projections

Previous research has evaluated the WRF model's performance, under similar configurations, and found that it is capable of resolving the fine-scale structure of storms and providing improved estimates of extreme precipitation (Zhang et al. 2009; Dulière et al. 2011). Nonetheless, the model does have biases which should be evaluated and corrected before using them as input to the hydrologic model.

To quantify and correct the WRF biases, we began by comparing the WRF simulations against surface weather observations taken from across the state (weather stations used in this analysis are listed in Appendix A). To account for elevation differences between WRF grid cells and the observations, we adjusted the observed temperatures based on an

Figure 2. Map of the annual average temperature biases for the WRF-OBS simulation. The left-hand map shows the biases for the annual average of daily minimum temperatures, while the right-hand map shows the same for maximum temperatures. The size of each circle denotes the bias, while the color denotes the sign of the bias.

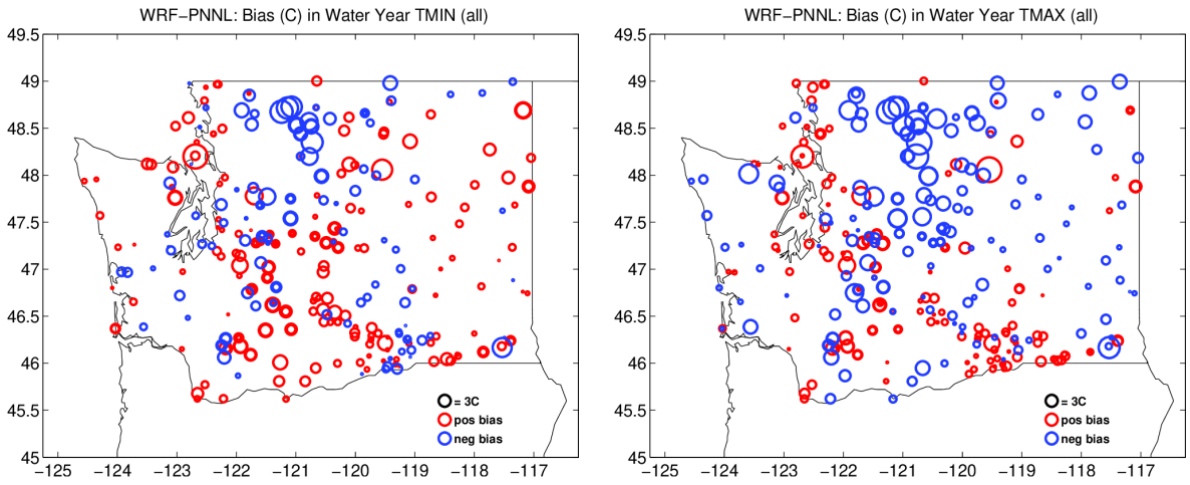

Figure 3. As in Figure 2 except showing the bias in annual total precipitation (left) and the top 1% of daily precipitation extremes (right).

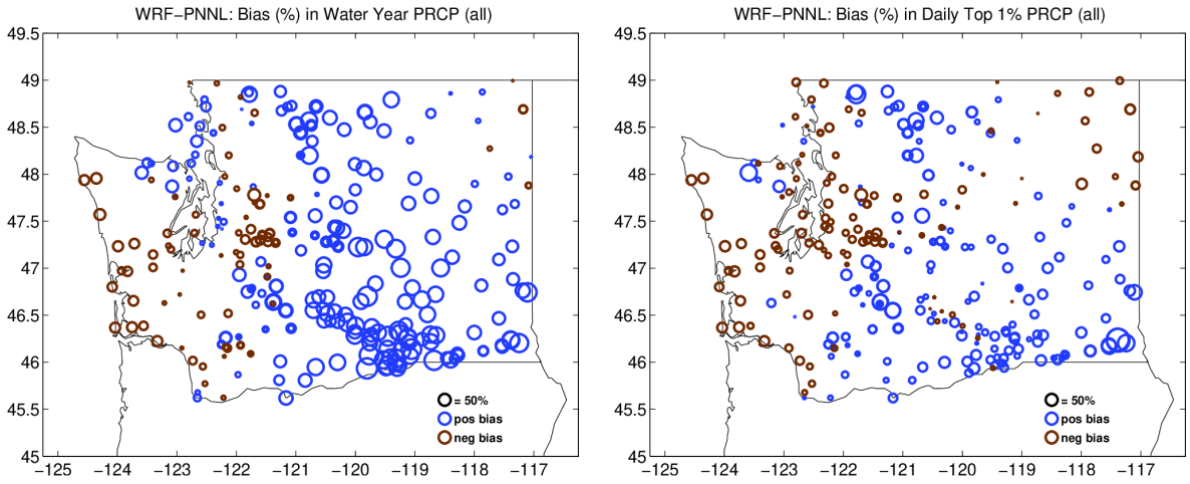

assumed lapse rate of 4.5ºC/km. Biases were calculated by comparing the average for the full WRF-OBS simulation (1981-2015) with the all valid observational data from 1970 to 2019, for each weather station. Figure 2 shows the comparisons for annual minimum and maximum temperatures. The patterns are difficult to discern, but there is a general pattern showing an insufficient diurnal range in WRF, where minimum temperatures tend to be too high and maximum temperatures too low. There also appears to be a consistent and substantial cold bias in the North Cascades. There is a much clearer pattern in the precipitation biases (Figure 3), generally showing that WRF precipitation tends to be too high in relatively dry parts of the state and too low in relatively wet parts of the state. The model also appears to be too dry to the east of the Olympic Mountains, ranging from the Kitsap Peninsula east to the crest of the Cascades, perhaps due to a bias in either the position or the intensity of the rain shadow in the lee of the Olympics.

The biases are similar for the WRF-GCM simulations. Since these include hindcast simulations, starting in 1970, we can evaluate these simulations in the same way as with the WRF-OBS simulation. For the WRF-GCM simulations, biases were estimated by averaging each WRF simulation for 1970-2015 and comparing them to the observational average for all years with valid data from 1970 to 2019. Bias maps for each model, for the variables shown in Figures 2 and 3, are shown in Appendix B.

Figure 4. As in Figure 2 except showing the bias in annual average wind speed (left) and incoming shortwave radiation (right).

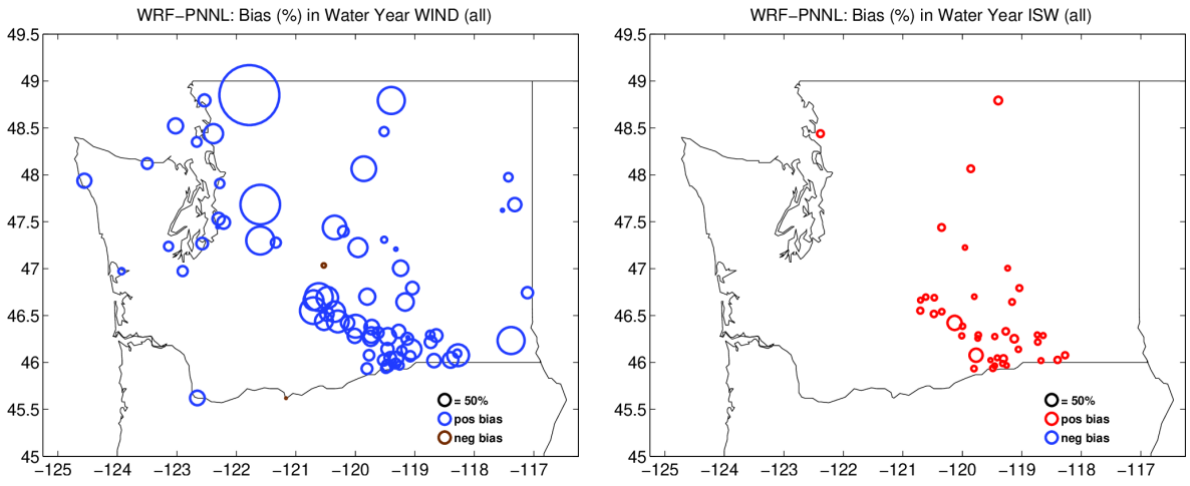

Some weather stations included measurements of wind and shortwave radiation (Figure 4). WRF overestimates both wind speed and incoming shortwave radiation everywhere in the state. Since neither of these datasets provide complete coverage, and noise in the observations could affect the bias measurements, we applied a uniform scaling based on the average bias among all comparisons across the state. These resulted in a scaling of 0.6 for all WRF wind estimates, and 0.9 for WRF shortwave estimates.

No observational comparisons were made for longwave radiation because very few observations exist. Instead, WRF longwave estimates were used directly from WRF without adjustment. Similarly, humidity estimates from WRF were not adjusted. Although observations are available, tests indicated that adjustments to humidity could frequently lead to over-saturated air or other physically implausible conditions. Future work could develop an improved approach, in which the relative humidity is corrected, then converted to vapor pressure deficit as used by the VIC model. Regardless of the approach, adjustments to humidity are unlikely to have a large effect on peak flow estimates.

The temperature and precipitation comparisons (Figures 2 and 3) make it clear that a uniform bias correction – in which

Figure 5. Comparison between PRISM and WRF-OBS, for the years 1981-2010, for annual total precipitation (top, ratio) and annual minimum (middle, difference in °C) and maximum temperature (bottom, difference in °C).

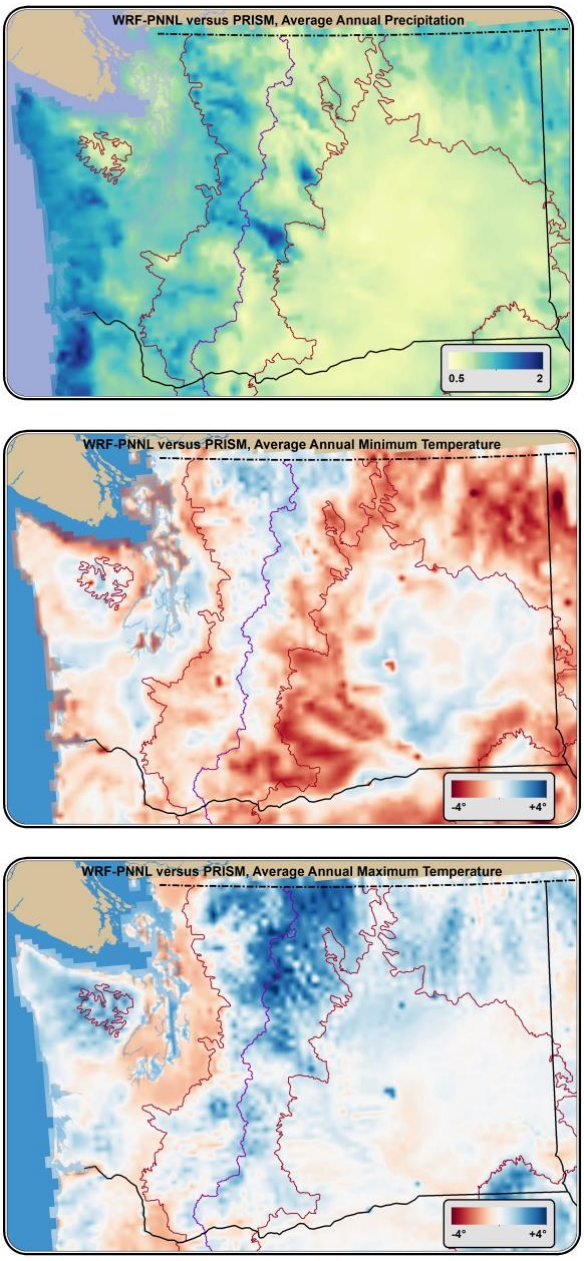

the same correction is applied to all grid cells – is not appropriate. Yet a spatially variable bias correction is challenging because it is not clear how the station-based biases could be extrapolated to provide coverage across the whole state. Recent work has developed an approach in which corrections are developed based on comparisons between WRF and observations at low elevations – where observations tend to be concentrated and topographic effects are minimized – and applied throughout (Bandaragoda et al., in review). Unfortunately, this method only works for a single watershed and it was beyond the scope of this work to expand the approach to the entire state. Instead we developed correction factors via comparison with results from the Parameter Regression on Independent Slopes Model (PRISM, 2004; Figure 5). Comparisons were made at the 1/16-degree resolution used by the hydrologic model (see following sections describing the model). The WRF data were bi-linearly interpolated to this resolution, while the PRISM results were aggregated from their native 30-arc-second resolution (1/120th-degree) to the 1/16-degree grid. The maps reflect the pattern shown in Figures 2 and 3 while providing correction factors for the full model domain.

Meteorological inputs for VIC were created by first interpolating the WRF data, via bi-linear interpolation, to the 1/16-degree VIC grid. Temperature and precipitation were then adjusted according to the values shown in Figure 5 (i.e.: scaled to adjust for the annual average bias), and wind and shortwave radiation were scaled by factors of 0.6 and 0.9, respectively. In all cases, the same scalings were applied to all time steps. The hourly WRF results were then aggregated to the 3-hourly VIC time step.

Hydrologic Model

Model Version

For this project, we are using the Variable Infiltration Capacity Model (VIC; Liang et al., 1994) version 4.2.d[1], which is the final release of classic VIC version 4, prior to the release of version 5 (Hamman et al., 2018). Version 5 uses the same physics, but is set up to work with a greater variety of inputs and is not backwards compatible with previous versions.

[1] https://vic.readthedocs.io/en/vic.5.0.1/Development/ReleaseNotes

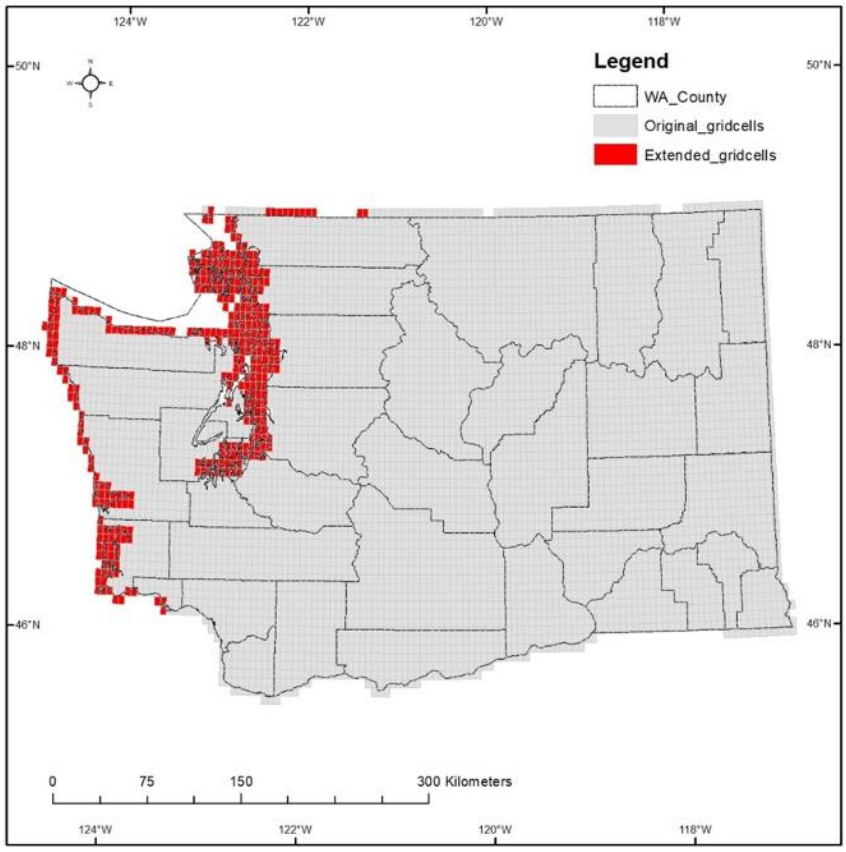

Figure 6. VIC domain, with new expanded domain highlighted in red. Grid cells are outlined to show the 1/16-degree spatial resolution of the model.

Grid Information and Soil Parameters

The model is run on the same 1/16-degree (about 5 x 7 km) grid used in previous studies (e.g., Hamlet et al. 2013; Chegwidden et al. 2019). The original soil parameter file contains 5,364 1/16-degree grid cells covering Washington State; these omitted a number of important coastal areas that were partially covered by water (Figure 6). We expanded the coverage to 5,711 grid cells by using Gridded National Soil Survey Geographic Database (gNATSGO, 2020) and extrapolating existing soil parameters via nearest-neighbor interpolation. The gNATSGO dataset is derived from a combination of the Soil Survey Geographic Database (SSURGO), State Soil Geographic Database (STATSGO2), and Raster Soil Survey Databases (RSS). The following VIC soil properties (for each layer) were updated using data from gNATSGO (Figure 7):

- Ksat: saturated hydraulic conductivity,
- bulk_density: bulk density of the soil,

- Wcr: the fractional soil moisture at the critical point, set as 70% of the field capacity,
- Wpwp: the fractional soil moisture at the wilting point, and
- Quartz: the quartz content of the soil.

The soil layer thicknesses were retained from previous work: 0.1 and 0.3 meter for first and second soil layers, while the thickness of the third layer is calibrated and varies across the state. The soil properties for each layer were retrieved from the gNATSGO dataset by using

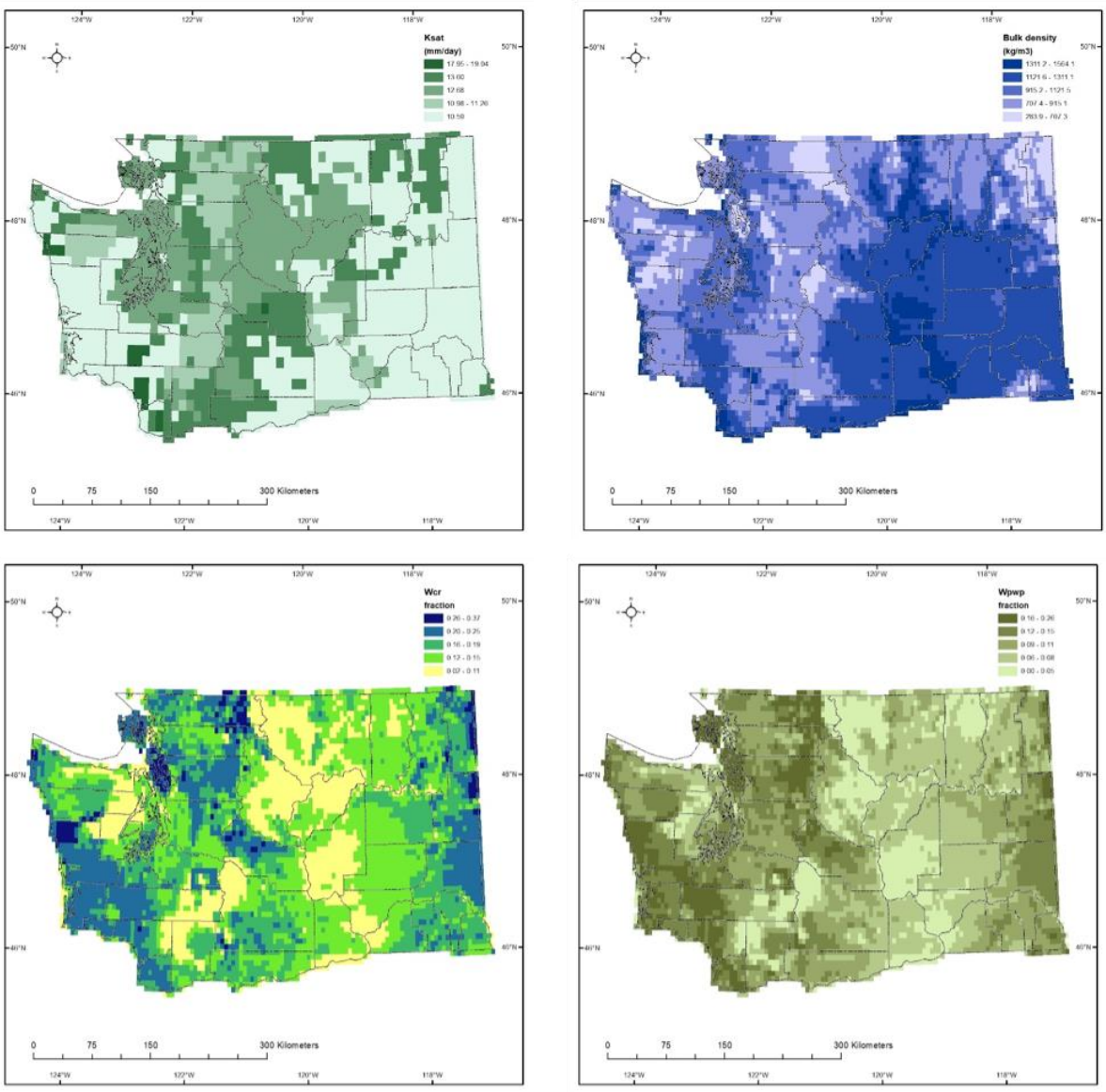

Figure 7. Soil properties obtained from gNATSGO (2020), shown here for the top soil layer.

its "Soil Data Development Toolbox" (ArcTools for ESRI ArcMap) and averaging values to correspond to the VIC soil layers: 0-10 cm for the first layer, 10-40 cm for the second layer, and the third layer was assumed to correspond to the average for 40-190 cm. Soil properties were obtained at a resolution of 10 m, then spatially averaged to the 1/16-degree VIC resolution.

Snowbands

The VIC model uses sub-grid elevation "bands" to model variations in snowpack within each grid cell. These were retained from previous work, described in Hamlet et al. (2013). For the new cells, these were primarily in coastal areas so only one snow band was used. Elevations were obtained from the Shuttle Radar Topography Mission 3 Arc-Second dataset (SRTM; NASA, 2013).

Land Cover

We updated the land cover based on National Land Cover Database 2016 update (NLCD[2]; Homer et al., 2020; Jin et al., 2019; Yang et al., 2018) and Moderate Resolution Imaging Spectrometer (MODIS) yearly Land Cover Type at 500 m resolution (MCD12Q1.005; Friedl et al., 2010). In the NLCD classification system forests are separated into three subgroups: deciduous, evergreen, and mixed forest. By using the MODIS landcover with the International Global Biosphere Project (IGBP) detailed classification system[3] in each VIC grid cell, the total fraction of NLCD forest is divided into Evergreen Needleleaf, Evergreen Broadleaf, Deciduous Needleleaf, and Deciduous Broadleaf forest. Mixed forest is kept as-is. The shrubland from NLCD is also divided into open and closed

Table 2. Land cover types used as input to the VIC model.

ID	Land Cover Type
1	Evergreen Needleleaf Forest
2	Evergreen Broadleaf Forest
3	Deciduous Needleleaf Forest
4	Deciduous Broadleaf Forest
5	Mixed Cover Forest
6	Woodland
7	Wooded Grasslands
8	Closed Shrublands
9	Open Shrublands
10	Grasslands
11	Crop land (corn)
12	Impervious surface
13	Pasture/Hay
14	Other lands

[2] https://www.mrlc.gov/data/nlcd-2016-land-cover-conus

[3] https://lpdaac.usgs.gov/news/modisterra-land-cover-types-yearly-l3-global-005deg-cmg-mod12c1

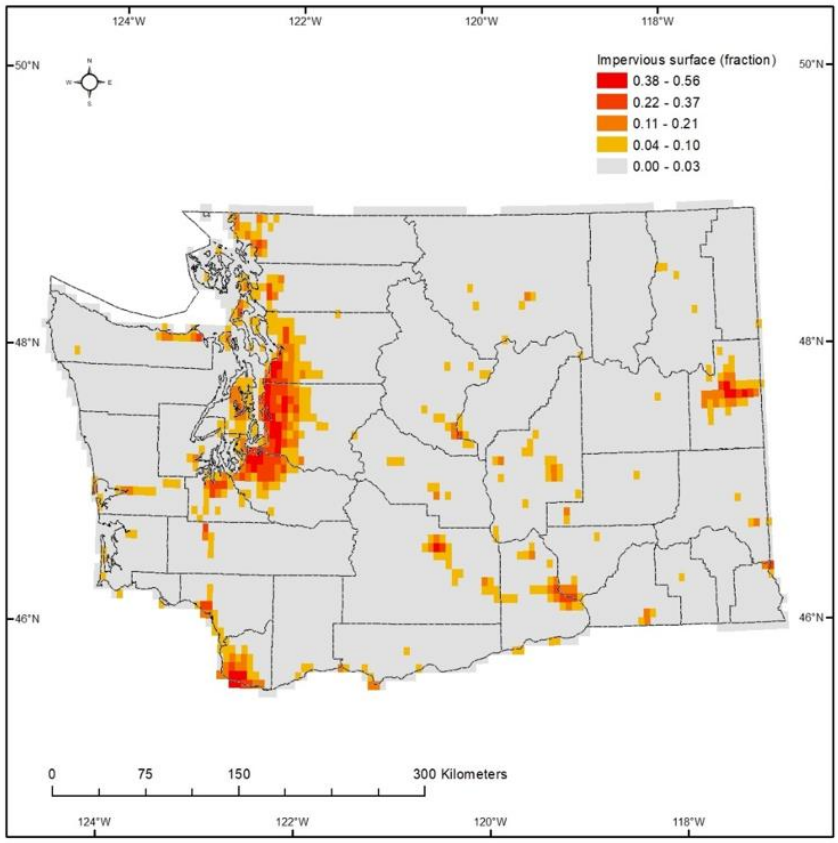

Figure 8. Fraction of impervious surface for each VIC grid cell.

shrublands depending on the fraction defined in the MODIS land cover product. The "developed" class in NLCD is first reclassified as Pasture/Hay because of its major component of lawn; then adjusted to remove the "Percent Developed Imperviousness", which is reclassified as impervious surface (Figure 8; all land cover types are listed in Table 2).

The monthly leaf area index (LAI) for each land cover portion within a VIC grid cell comes from the Project for On-Board Autonomy – Vegetation (PROBA-V) 300 m LAI dataset (version 1.0; Fuster et al., 2020). Data were averaged from 10 days to monthly for the years 2015-2017. We obtained the average LAI for each land cover type by overlaying the MODIS 500 m resolution land cover with the mean monthly LAI and aggregating both up to the 1/16-degree VIC grid resolution. There are no LAI data available for certain land cover types and VIC grid cells. In these cases we used the average monthly LAI over Washington state. For impervious surfaces we set the monthly LAI to zero.

VIC Calibration

The purpose of this project is to develop grid cell-by-grid cell estimates of culvert sizing for all of Washington State. This poses a challenge because the observations that are needed for calibration do not cover all areas of the state. This means that a "global calibration" is needed, in which parameters are optimized for certain basins and then generalized to the region. We accomplish this by focusing on high-quality unregulated streamflow observations from across the state and optimizing model parameters separately for each of three ecoregions, as described below.

Streamflow observations

We downloaded historical streamflow observations from USGS National Water Information System (NWIS[4]), which contains 1,041 gauges within Washington state for the years 1902

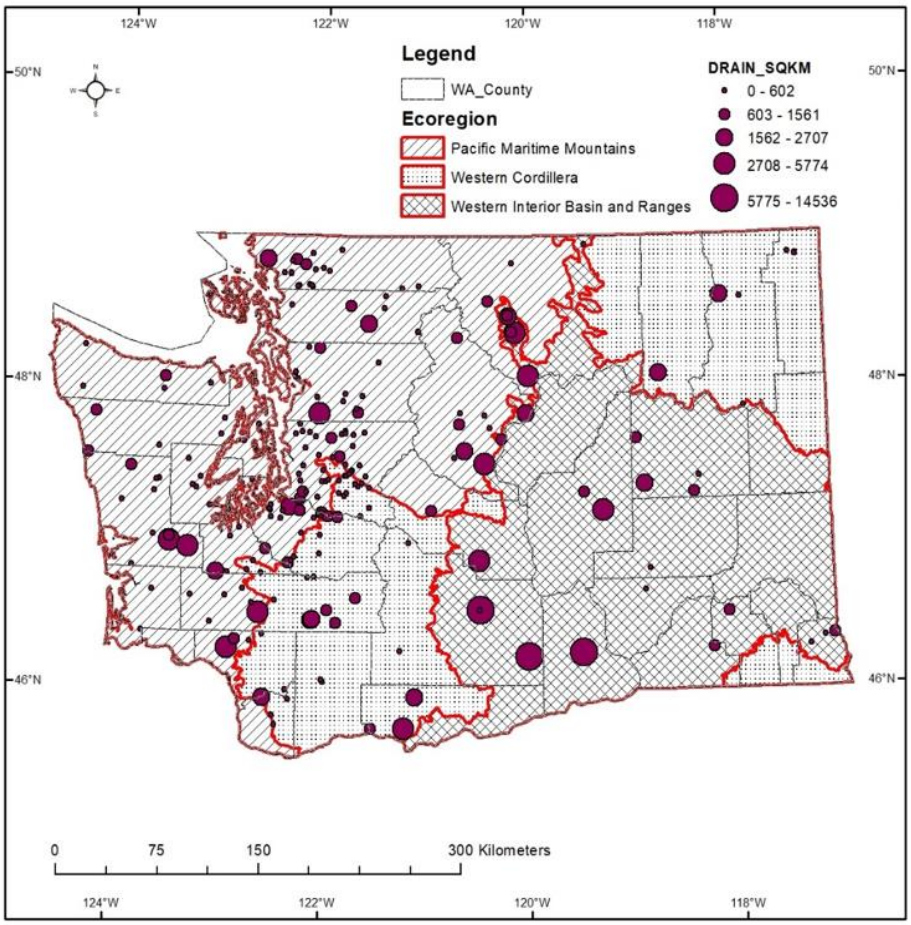

Figure 9. Stream gauges and ecoregions used in model calibration. The size of the dot for each gauge denotes the corresponding drainage area. The ecoregions are the same ones used in the bankfull width calculations.

through 2020. From these 1,041 gauges we selected 218 gauges having at least two years of observations within the 1970-2015 time period of the historical simulation (Figure 9; Appendix C).

To compare the historical VIC results with the stream gauge observations, the 3-hourly results were first aggregated to daily, then averaged over all grid cells within the drainage basin upstream of each stream gauge. The spatial averaging is weighted to account for the fractional overlap between each grid cell and the drainage basin in question. The averaging does not account for flow routing and instead assumes there is no time lag between each grid cell and flows at the downstream gauge location – this is justified at a daily time step for the relatively small basins used in our calibration (culvert catchments range from well under a square mile to a few square miles at most). Although a number of metrics were tested (e.g., annual 7-day minimum flows), we ultimately chose to focus the model ranking on the daily flow comparisons in order to maximize the sample size available for evaluation.

Soil Parameters used in Model Calibration

The VIC soil parameters include watershed-scale hydrologic properties that either cannot be measured directly or have significant spatial variations. These need to be calibrated by iteratively comparing simulated results against observations. The following five soil parameters were calibrated in the current study:

Table 3. Ranges used for each soil parameter used in calibration.

Parameter	Range	Unit
BI	0.001 – 0.4	N/A
$D_{s,MAX}$	0.01 – 30	mm/day
D_s	0.0001 – 1.0	fraction
W_s	0.01 – 1.0	fraction
D2	0.001 - 3	m

1. BI: Parameter controlling the shape of variable infiltration capacity curve;
2. $D_{s,MAX}$ is the maximum baseflow from the lowest soil layer;
3. D_s is the fraction of $D_{s,MAX}$ where non-linear baseflow begins;
4. W_s is the fraction of the maximum soil moisture (of the lowest soil layer) where non-linear baseflow occurs; and,
5. D2 is the soil depth of the lowest soil layer.

These are the standard VIC parameters used for calibration.

Based on soil physics, literature, and earlier VIC calibrations over the Columbia River Basin (e.g., Hamlet et al., 2013), we identify the range of plausible values for each of these soil

Table 4. The 40 parameter sets used in model evaluation.

Sets	BI	$D_{s,MAX}$	D_s	W_s	D2	Sets	BI	$D_{s,MAX}$	D_s	W_s	D2
0	0.10	1.88	0.46	0.15	2.96	20	0.40	21.38	0.39	0.64	1.31
1	0.09	5.63	0.41	0.47	1.91	21	0.25	4.88	0.71	0.05	1.01
2	0.39	28.88	0.24	0.74	0.94	22	0.02	8.63	0.01	0.72	2.59
3	0.19	16.88	0.11	0.69	2.51	23	0.22	29.63	0.76	0.86	2.29
4	0.15	25.88	0.56	0.34	0.34	24	0.16	17.63	0.44	0.12	1.69
5	0.31	2.63	0.91	0.22	0.86	25	0.18	15.38	0.69	0.84	2.89
6	0.07	10.88	0.96	0.39	1.46	26	0.06	12.38	0.66	0.81	0.26
7	0.24	7.88	0.09	0.99	1.16	27	0.32	23.63	0.61	0.07	0.49
8	0.29	16.13	0.04	0.25	1.76	28	0.11	19.88	0.86	0.96	1.54
9	0.13	13.13	0.06	0.29	1.09	29	0.23	20.63	0.74	0.57	1.99
10	0.08	11.63	0.16	0.59	2.14	30	0.03	0.38	0.81	0.91	1.39
11	0.35	25.13	0.54	0.94	0.64	31	0.21	9.38	0.29	0.76	2.21
12	0.38	3.38	0.84	0.02	0.71	32	0.28	24.38	0.51	0.17	0.79
13	0.04	6.38	0.99	0.27	2.81	33	0.36	14.63	0.21	0.37	2.44
14	0.30	4.13	0.34	0.67	1.84	34	0.26	28.13	0.79	0.49	0.11
15	0.37	18.38	0.19	0.62	2.74	35	0.34	27.38	0.64	0.79	0.56
16	0.27	22.88	0.94	0.42	1.24	36	0.12	7.13	0.89	0.44	0.04
17	0.17	13.88	0.31	0.10	2.36	37	0.01	26.63	0.59	0.89	0.41
18	0.14	22.13	0.49	0.20	0.19	38	0.33	10.13	0.36	0.52	1.61
19	0.20	19.13	0.14	0.32	2.66	39	0.05	1.13	0.26	0.54	2.06

parameters (Table 3). Based on these ranges, we generated 40 parameter sets using Latin hypercube designs with "center" criteria (Table 4; python package pyDOE[5]). These parameter sets were the basis of the model evaluation, described below.

Evaluation Metrics

We based our ranking on the Nash-Sutcliff model efficiency (NSE) coefficient calculated from the natural log of the observed and modeled flows ("NSE-log"):

$$\mathrm{NSElog} = 1 - \frac{\sum_{t=1}^{T}(\ln(Q_m^t) - \ln(Q_o^t))^2}{\sum_{t=1}^{T}\left(\ln(Q_o^t) - \overline{\ln(Q_o)}\right)^2} \qquad \text{Eq. 2}$$

[5] https://pythonhosted.org/pyDOE/randomized.html

where $\overline{\ln(Q_o)}$ is the mean of observed log-discharges, and Q_m^t and Q_o^t are modeled and observed discharge at time t (here we use a daily time step), respectively. The standard NSE is dominated by biases in peak flows; the logarithmic transformation ensures that model performance is evaluated across more than simply the largest flows. In particular, this ensures that model ranking is also influenced by the model's ability to reproduce low flows.

We also evaluated results for the standard NSE and Pearson correlation (r). We did not deem the correlation-based rankings reliable since these are biased high due to the seasonal cycle in flows and therefore not very sensitive to biases. Rankings were different for each metric, but the rankings for NSE bore many similarities to those based on NSE-log.

Ranking of soil parameter sets

As noted above there is no way to calibrate the model independently for every grid cell across the entire state. Instead we use ecoregions as the calibration unit (Figure 9), selecting the soil parameter sets that best represent flows for the gauges within each ecoregion. Stream gauge sites with dams upstream were excluded, and only sites with <1% irrigated fraction were included in the analysis. Sites with a dam upstream were also excluded.

We tested multiple ways of ranking the performance of each of the 40 soil parameter sets. In general, these fell into four categories of approaches:

1. Select the highest scoring parameter sets (greatest NSE-log for the greatest number of gauges within the ecoregion)
2. Select the parameter sets that most frequently out-performed other parameter sets (that consistently outrank other parameter sets),
3. Select the parameter sets with the least number of low scores, or
4. Select the parameter sets with the best median score.

The latter two approaches were based on the observation that some parameter sets performed very well for certain gauges yet very poorly for others. Our aim is to optimize the performance across the entire region rather than maximize it only for certain sites. After evaluating each, we chose to base our rankings on the median score across all sites in each ecoregion. There were similarities in the rankings across each of these approaches, but selecting based on the median score exhibited the most consistent improvements when compared against the average performance for all 40 parameter sets.

Streamflow comparisons are just one way to evaluate model performance. In selecting top parameter sets, we applied one additional constraint: we only selected parameter sets for which the bias in annual average evapotranspiration (ET) was less than 50%, based on a comparison with ET estimates derived from FLUXNET observations (using Model Tree Ensembles, or MTE; Jung et al., 2010). This constraint was added after model testing

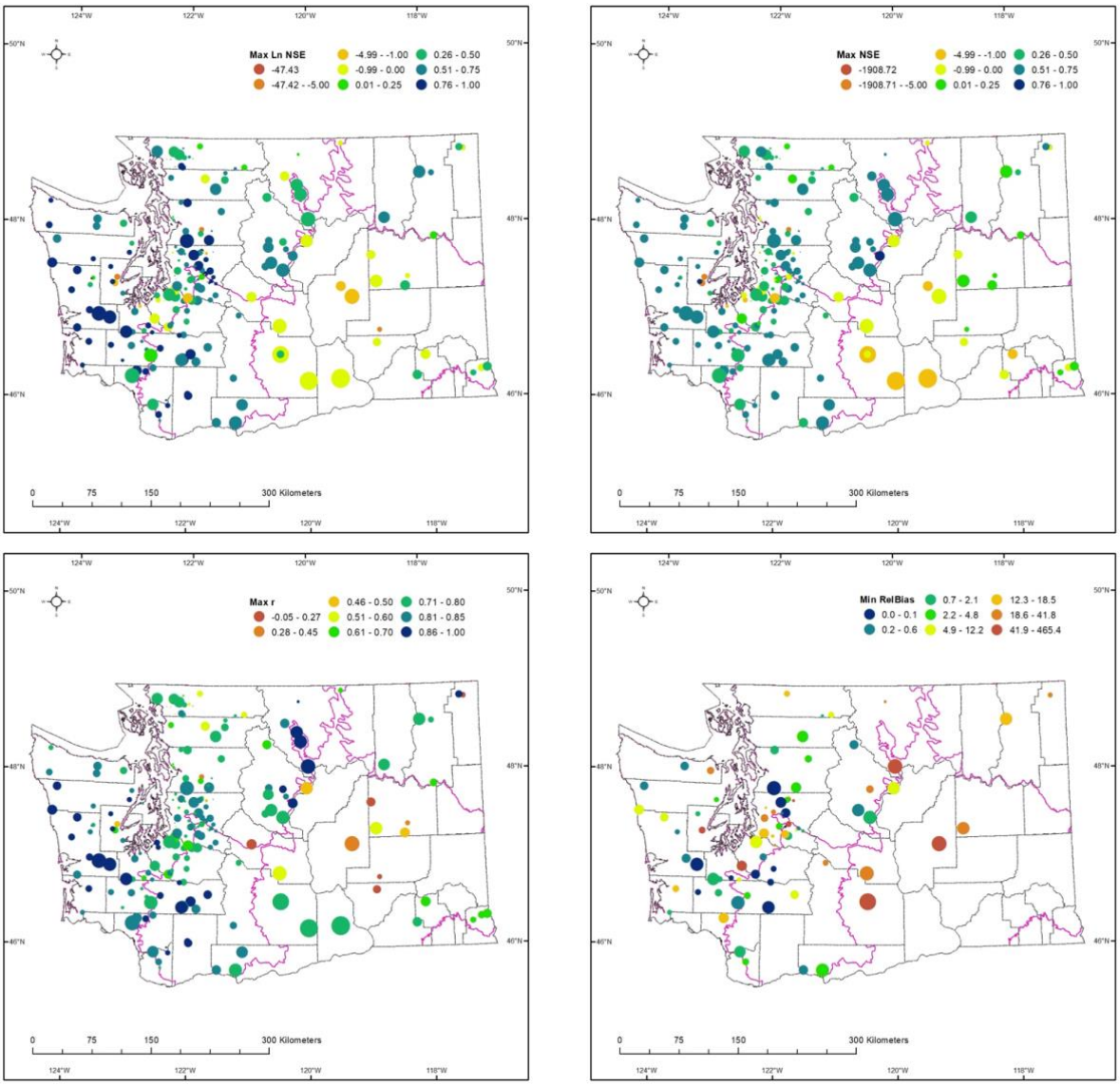

Figure 10. Top-scoring parameter set for each streamflow site, for NSE-log (top left), NSE (top right), correlation (bottom left), and relative bias (bottom right).

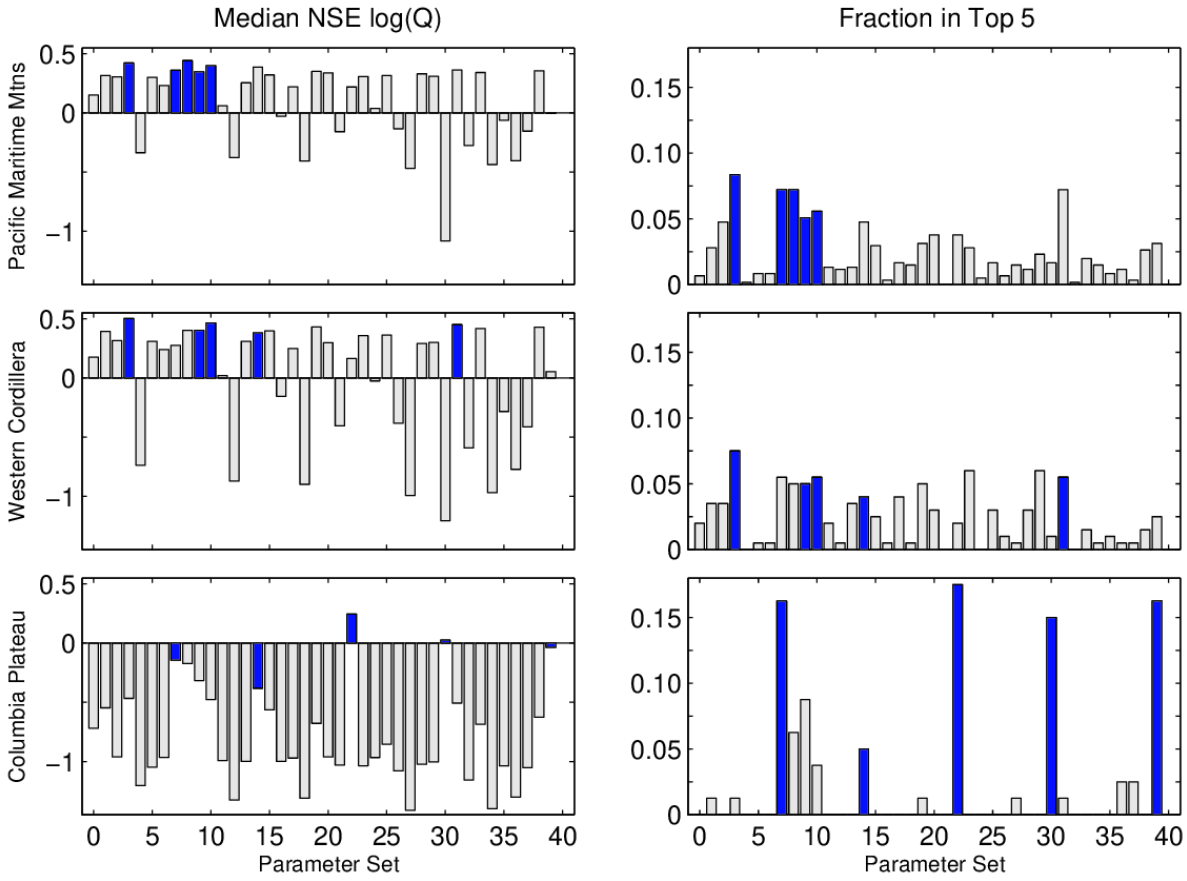

Figure 11. Median NSE-log across all sites in each ecoregion (left), and fraction of sites for which each parameter set had one of the top 5 scores (right). Rows show results for each ecoregion: Pacific Maritime Mountains (top), Western Cordillera (middle), and Columbia Plateau (bottom).

revealed that some parameter sets could be highly ranked yet dramatically overestimate soil infiltration rates. This resulted in substantial underestimates of ET as a result of unrealistically rapid infiltration in the soil column, and could have a resulting impact on flood peaks and the associated sensitivity to climate change.

Figure 10 shows the results for the best-scoring parameter set for each stream gauge site across the state, and Figure 11 shows the NSE-log scores for each parameter set. These results show that streamflow is relatively well captured by the model for most of the state. The exception is the Columbia Plateau, where the model appears to dramatically

overestimate flows. However, even for the Columbia Plateau, modeled flows correlate fairly well with the observations at most sites.

We selected the top 5 parameter sets for each ecoregion (Table 5), based primarily on the median NSE-log score for each ecoregion. In our analysis, we calculated the median flow estimate among the 5 parameter sets, using that as a best estimate of hydrologic conditions.

Table 5. Top 5 parameter sets selected for each ecoregion.

Ecoregion	Param. Sets
Pacific Maritime Mountains	3,7,8,9,10
Western Cordillera	3,9,10,14,31
Columbia Plateau	7,14,22,30,39

Post-Processing and Analysis

Using Modeled Flows to Estimate Bankfull Width

The VIC model outputs are listed in Table 6; streamflow is derived by summing runoff and baseflow. As in previous work, we estimate bankfull width using the empirically-based equations developed by Castro and Jackson (2001; Eq. 2, Table 1, Figure 1; Omernik, 1987).

Peak Flow Statistics

We computed extreme statistics from the water year maxima in streamflow. These maxima correspond to the 3-hourly VIC time step used in the simulations. Past evaluations show a high correlation between 3-hourly and instantaneous flows, suggesting that our analysis can be interpreted as representative of the change in instantaneous peak flows.

To calculate extreme statistics, the Extreme Value type 1 distribution described by Gumbel (EV1), the Log-Pearson type 3 (LP3), and the generalized Extreme Value (GEV) distribution with L-moments are commonly used. In this study we apply the GEV distrib-

Table 6. Output variables from VIC simulations. These are produced separately for each grid cell in the domain. All units are in mm per time step.

Name	Description
OUT_PREC	Precipitation
OUT_PET_SHORT	Potential evapotranspiration of a short reference crop (Alfalfa)
OUT_SWE	Snow water equivalent
OUT_EVAP	Total net evaporation
OUT_RUNOFF	Surface runoff
OUT_BASEFLOW	Baseflow out of the bottom soil layer
OUT_SOIL_MOIST0	Soil moisture content, top layer
OUT_SOIL_MOIST1	Soil moisture content, middle layer
OUT_SOIL_MOIST2	Soil moisture content, bottom layer

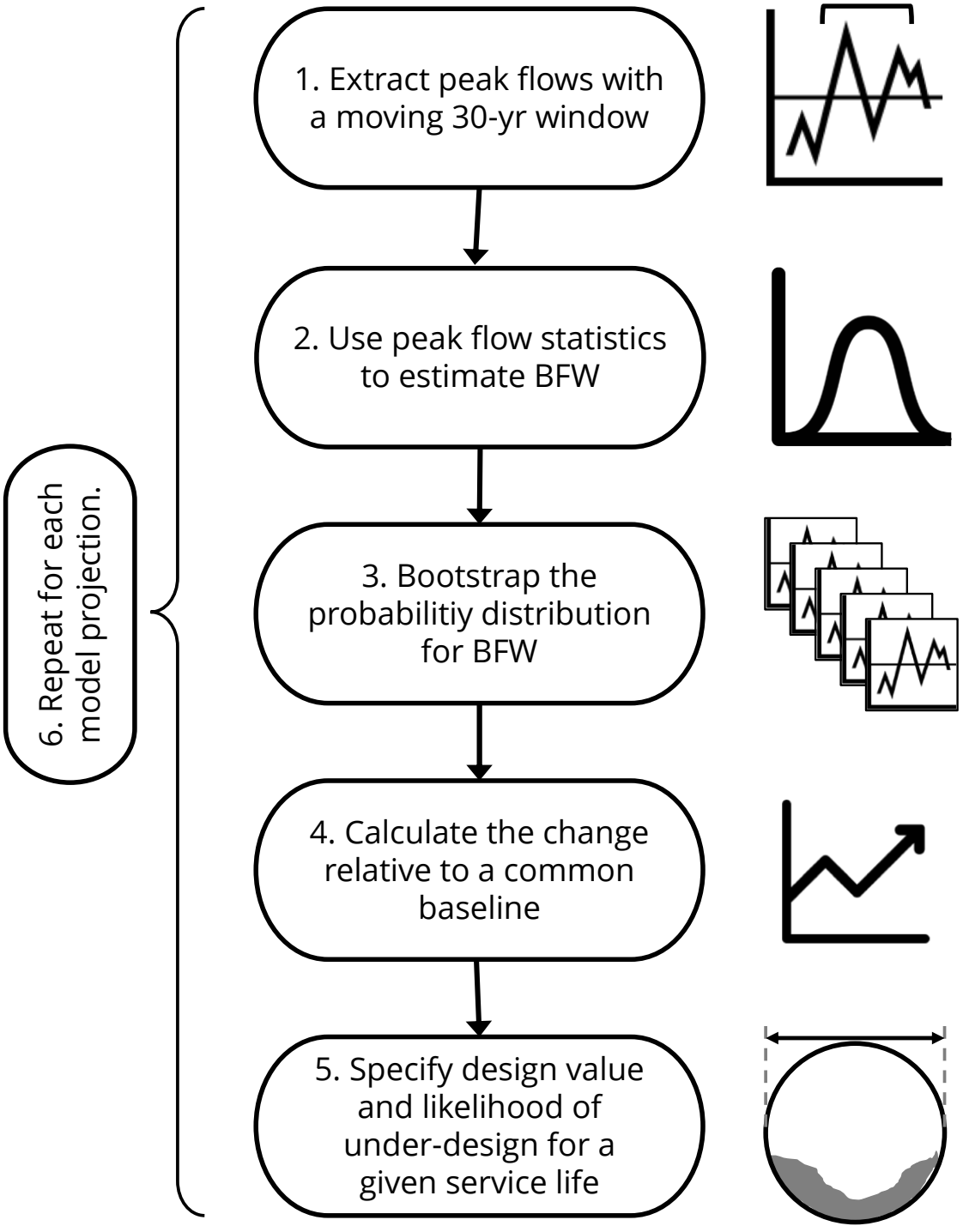

Figure 12. Schematic illustration of the approach used to estimate changes in bankfull width.

ution with L-moments to estimate extreme precipitation statistics – following the methodology described in Salathé et al. 2014 and Tohver et al. 2014 – based on findings that indicate it is superior to the LP3 distribution (Rahman et al. 1999 & 2015, Vogel et al. 1993, Nick et al. 2011).

Monte Carlo Resampling

We use a bootstrap approach to capture the uncertainty in the peak flow statistics by resampling 1,000 times, with replacement, from each historical and future time period. Tests indicated that 1,000 samples were sufficient to adequately represent the empirical probability distribution in extreme flow statistics. As in Wilhere et al. (2017), we use projected future bankfull flow to estimate future bankfull width based on Castro and Jackson (2001; Eqn. 2, Table 4).

In order to minimize the effect of model biases on the projections, we consider only the percent change in future flows relative to a historical baseline. By considering only the relative change we remove any absolute biases that may be present in the model streamflow estimates. For the historical period we use 1970-2015 while for each future period we follow the convention of using 30-year periods (2020-2049, 2030-2059, 2040-2069, 2050-2079, 2060-2089, 2070-2099). The 30-year future periods are a compromise between the need to detect changes over time and minimize the sensitivity to random short-term variability. Since geomorphic change (change in bankfull width) is likely to lag changes in flows, we suggest considering the final year in each time frame as the representative year for each projection (e.g., results for 2020-2049 provide the estimated bankfull width for 2049).

The result is a separate estimate of the percent change in bankfull width for each bootstrapped sub-sample; i.e.: 1,000 percent change estimates for each future time period. This process, outlined in Figure 12, is repeated separately for each VIC simulation (there are a total of 60 VIC simulations: 12 GCM-WRF projections x 5 VIC parameter sets).

Translation to Design and Risk Assessment

Wilhere et al. (2017) suggest using two statistics for climate-adapted culvert design: (1) the average percent change in BFW, among all climate model projections, and (2) the number of models projecting an increase in BFW. The ensemble of GCM projections available to us

is not equivalent to a random sample in the statistical sense – in particular because the models are not independent. As a result, the range among models cannot be easily translated to a probability distribution for future conditions (Knutti, 2010; Stephenson et al.,2012). Instead, the most credible ways to communicate uncertainty are often the simplest (Kandlikar et al., 2005). Wilhere et al. (2017) adopted perhaps the simplest measure of uncertainty − the number of models that agree on the sign of change (Kandlikar et al., 2005; Tebaldi et al., 2011). Their scheme provides three vital pieces of information: the direction of change (increase or decrease in BFW), the expected magnitude of change, and an indicator of the certainty/uncertainty of change.

Quantitative definitions of risk often possess two components: magnitude of damage (or of cost) and the uncertainty (or probability) that damage of a particular magnitude will occur. Hence, Wilhere et al. (2017) developed a scheme for defining "actionable" risks (i.e., estimated risk to fish is large enough to warrant action) based on proxies for magnitude of damage and uncertainty: the mean future increase in BFW is >*X*% and at least *Y* of the 10 models project an increase in BFW. These proxies would be calculated for the time period corresponding to a culvert's expected service life. In their example, an actionable risk was a mean future increase in BFW >5% and at least 6 of the 10 models projecting an increase in BFW. Their scheme is one way to inform decisions regarding climate-adapted culverts. However, some decision makers may prefer a more intuitive risk statistic, such as the probability of incurring a given cost or the probability that an unacceptable event will occur. This is why we developed a complementary probabilistic approach to analyzing the projections.

Our probabilistic approach provides the probability that a culvert will be too narrow sometime in the future because channel width has increased due to climate change. We assumed that an adequate culvert width must be equal to or greater than a stream simulation culvert width (Equation 1), and calculated future adequate culvert widths using projected future channel widths We estimated probabilities using our bootstrapped samples, by simply taking the fraction of bootstrapped sub-samples that result in projected future adequate culvert widths that exceed a culvert's proposed width. We evaluated these changes for the full expected service life of the proposed culvert, calculating culvert widths from bankfull flows using Equations (1) and (2) (see Background section of this report).

For example, a user may want to know the probability that future bankfull widths will lead to an undersized culvert if a culvert is designed with the current bankfull width (i.e., not climate adapted) and the culvert has an expected service life is 50 years. In this case, the 1,000 bootstrapped estimates will be lumped together for the 2030, 2040, 2050, 2060, 2070 time periods (i.e., 50 years). From these 5,000 bootstrapped estimates of percent change in BFW, the fraction that project a future desired culvert width greater than the proposed culvert width gives the probability of the culvert being too narrow at some time during it's expected service life . This calculation can be repeated for any culvert width of interest, for service lifetimes ranging from the present to 2099.

This approach is based on the probabilistic methodology developed by Byun and Hamlet (2020). Our approach is distinct from Byun and Hamlet (2020) in two respects. First, the Byun and Hamlet (2020) projections are based on statistical downscaling, which previous studies have shown may not adequately capture changes in extreme precipitation (e.g., Salathé et al., 2014). As described above, our projections are based on a new ensemble of dynamically downscaled projections, and the hydrologic model was calibrated using a historical simulation produced with the same regional climate model (Chen et al., 2018). Second, Byun and Hamlet (2020) do not account for sample bias in the global model projections – in their approach, a single 30-year period is used to produce the statistically downscaled projections from which the extreme value fit is produced. In our approach each 30-year period is sub-sampled, resulting in a probability distribution that is less sensitive to outliers.

Web Tool and Data Access

Site-level information on hydrology and geomorphology is essential for the design of any in-stream hydraulic structure. Designing climate-adapted culverts requires projections of *future* hydrology and geomorphology. Hence, this project's main objective is to develop an internet site that provides engineers with up-to-date site-level projections of future changes in stream discharge and channel width caused by climate change.

Prior to receiving the grant from the Northwest CASC, WDFW developed an intranet site to provide its field staff with projections of future changes in bankfull width, bankfull flows, and 100-year flood flows. These projections came from the work of Wilhere et al. (2017). WDFW staff shared this information with culvert project proponents and designers who

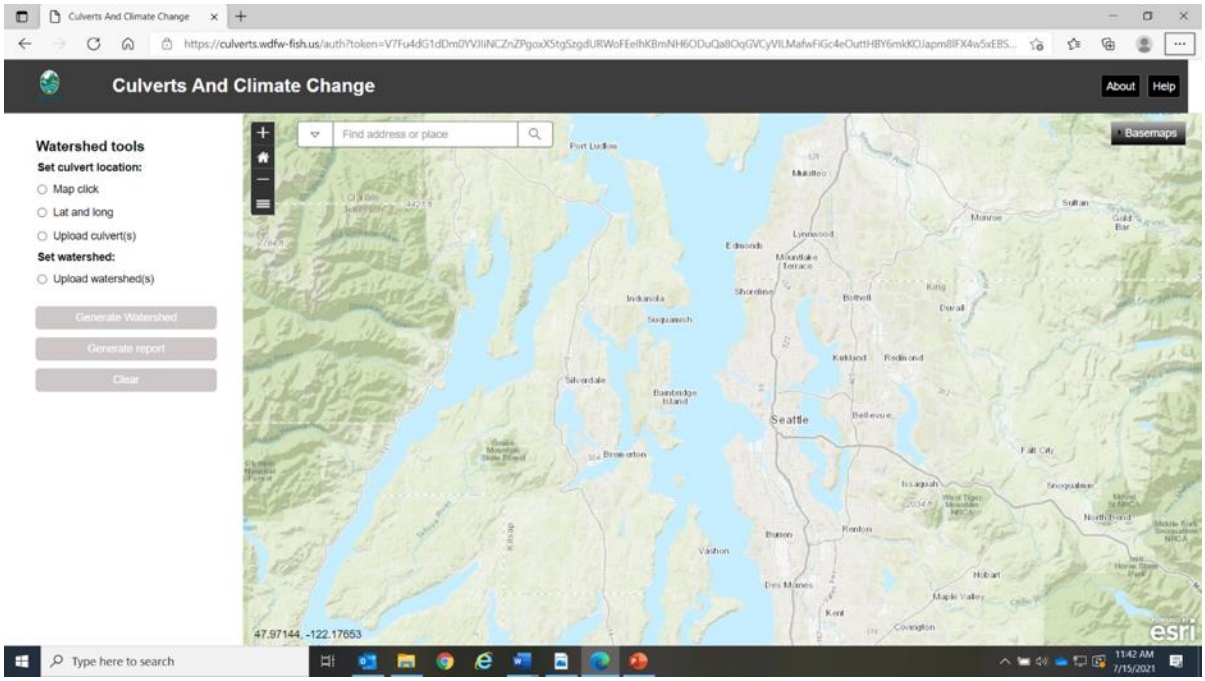

Figure 13. Screenshot of the current Culverts and Climate Change internet site.

were interested in climate-adapted culverts. We soon recognized that the public should have direct access to this information. A primary focus of the current work was to migrate WDFW's intranet site to the internet (Figure 13).

An important step in the intranet to internet migration was asking our clients, i.e., culvert project proponents and culvert designers, what they needed and wanted from an internet site for climate-adapted culvert design, or for the design of any climate-adapted in-stream hydraulic structure. To better understand user needs, we hosted a half-day workshop on October 11, 2019 in Olympia, Washington to query potential users of the internet site. The workshop was attended by 17 people from county governments, other state agencies, a public utility, and private consulting firms; all of them interested in climate-adapted culverts. We explained the internet site and the science supporting it, gave a demonstration, and asked them to complete a hands-on exercise using the tool. The workshop ended with their impressions and ideas to make the internet site more useful and user-friendly (Table 7).

An original objective of this project was to provide projections of future changes in 5, 10,

Table 7. Select list of suggestions for improvements to Culverts and Climate Change internet site from participants in October 2019 workshop.

Map Features
A map or background layer that shows where no BFW projections are available
Show where a selected culvert location is relative to the whole state [*an inset map of Washington?*] -- on output map only
Include a base map that replicates [*links to?*] the FPDSI maps so we could click on a culvert.
Ability to search by city, county, street intersection, or stream name, and by WDFW FPDSI #
Ability to search by lat & long in the search box
look at StreamStats internet site for ideas about user interface – lay out, bells and whistles, aesthetics, format of output, options for results download
Add USGS 7.5' topo map in the base layers
% change grid as background layer (similar to map in report)
show map scale (1:x) on map
Watershed Delineation Features
manually delineate your own watershed
An UNDO button for watershed boundary editor
Map click should display lat & long of culvert location
Output Features
Provide other hydrologic data in the report (i.e., tool output)?: % change in 50, 20-yr flows (?), and low flows
Ability to export the watershed as a shape file
Add "about" information to the report (i.e., output) page – people sometimes include the report page as an appendix, good to have complete reference information on report page
give lat & long of culvert location in the pdf report; give map scale (1:x) on report too
Report should include a software version # and date of hydrological projections. If the projections are updated, we'll want to know what version we are working with.
Majority liked the display of the probability prototype Guillaume presented. Thought it made it clearer to present to a manager and be able to convey the importance of addressing climate.
Liked being able to put in your proposed design [*culvert width*] and see how it does over time.
Help Features
Give some troubleshooting tips on Help page. Example: "try resetting the pin upstream if watershed delineation doesn't work at first"
Display tips for common next steps in info bar at bottom of page
Add current equation for stream sim. On a new FAQ page
Can we "peek behind the curtain"? Show what were the inputs? How did you get from watershed to BFW? Maybe a flow chart or decision tree. Gives you confidence if you have to explain it to somebody else.
On Help page clarify that you need to have both Pin and watershed selected to "generate watershed"
Other Features
Process multiple culvert locations sequentially as a "batch." Output results entire batch in a single file.
change spatial data from shapefile to file geodatabase

25, 50, and 200-year peak discharges through the same online tool. However, workshop participants expressed little interest in such peak discharge information. Instead, tool updates were focused on incorporating nearly all suggestions from the workshop into the Culverts and Climate Change internet site. If a demand does arise for information on future changes to various peak discharges, these data are available and can be incorporated via the same process used to incorporate the bankfull flow projections.

Migrating the Culverts and Climate Change intranet site to the internet raised concerns about cyber security. One major concern was that an external user could access the site numerous times simultaneously (either accidentally or intentionally), initiate numerous reports simultaneously, and thereby crash the system. In particular, we were concerned about crashing the ArcGIS server which many people in WDFW depend upon. To address this concern Secure Access Washington (SAW) was utilized as the pubic-facing interface for the internet site (Figure 14). Directions for accessing the Culverts and Climate Change internet site through SAW are provided in Appendix D.

Within the Culverts and Climate Change internet site, site-specific projections of future changes in bankfull width, bankfull flow, and 100-year peak flow are produced in six steps. First, the entire drainage area upstream of a culvert's location is delineated. This was accomplished via a flow-direction grid that was created for all of Washington State with the ArcGIS hydrology toolset using 10-meter digital elevation models and stream flowlines from the National Hydrography Dataset. If this automated process produces an inaccurate watershed boundary, then the internet site enables the user to

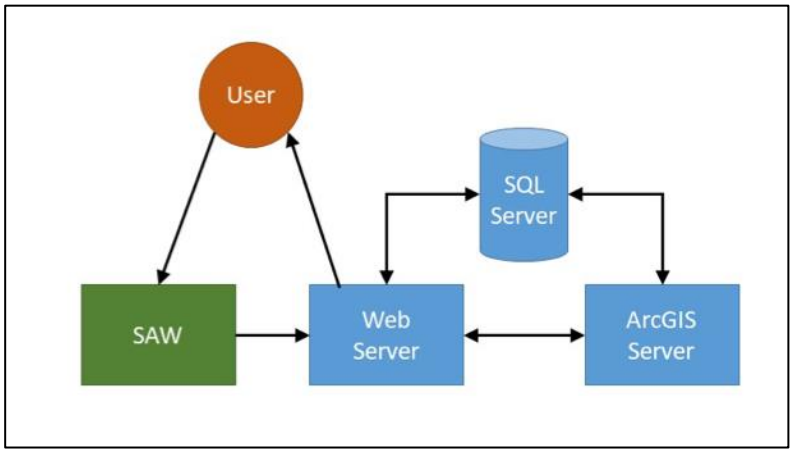

Figure 14. Internal structure of Culverts and Climate Change internet site. Secure Access Washington (SAW) provides a secure interface between the internet site and users. The Web, ArcGIS, ad SQL servers are maintained by WDFW. The ArcGIS server provides functions for spatial analysis, and the SQL server provides data storage and database functions.

manually edit the boundary. Second, the areas of intersection between the drainage area and the grid cells are determined. Third, the projected bankfull discharge at the culvert location is calculated as an area-weighted average of the bankfull discharges of the grid cells intersecting the drainage area. For a given time period, that calculation is repeated 24 times − for future projections from each of the 12 GCMs and for the 12 historical simulations corresponding to each of the GCMs. Fourth, using hydraulic geometry equations (Equations 1 and 2), the 24 bankfull flows are used to calculate bankfull widths. Fifth, the percent change between projected future bankfull width and historical bankfull width is calculated for each of the 12 GCMs. And finally, the mean projected percent change in bankfull width is estimated. Similar computations are used to obtain the projected future percent change in bankfull flow and projected future percent change in 100-year peak flow.

The internet site displays projections for future percent changes in bankfull width, bankfull flow, and 100-year peak flow in a report format that can be exported to a PDF file (Figure 15). The report shows the watershed boundary on a small map, with two graphs showing the projected percent change in BFW and percent change in 100-year peak flow for all 12 GCMs. The range among these 12 models provides an estimate of the uncertainty. To apply the results in culvert design, the bankfull width at the culvert site is estimated by the user, typically via a field survey, and the

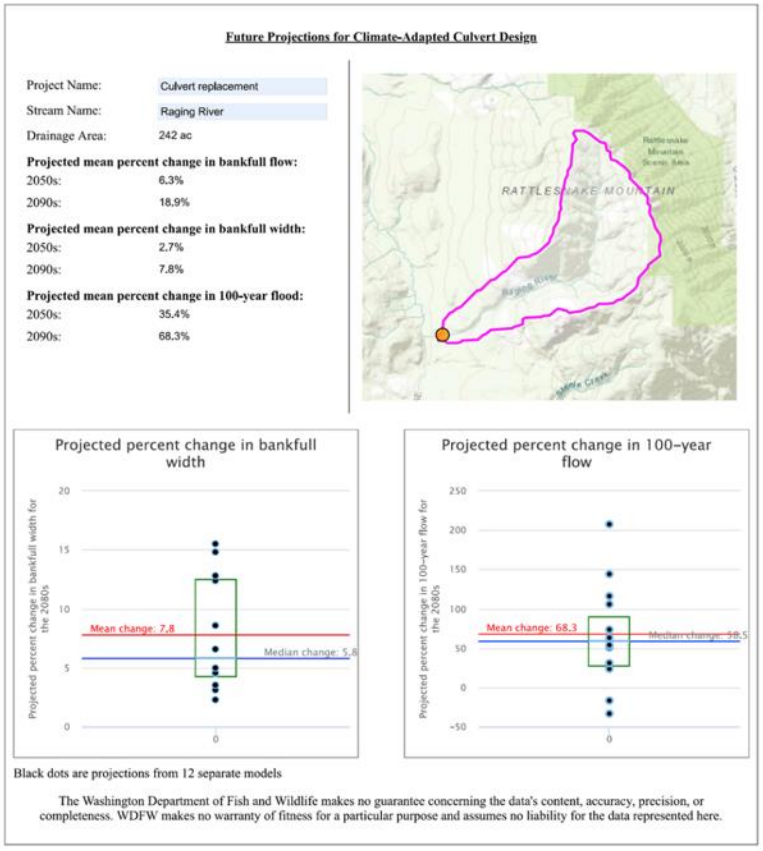

Figure 15. Report providing projected future percent changes in bankfull width, bankfull flow, and 100-year peak flow produced by Culverts and Climate Change internet site.

projected mean percent change in bankfull width is applied to the measured bankfull width. This yields the expected future bankfull width at the site.

The revised Culverts and Climate Change internet site (Figure 16) provides a probabilistic characterization of the projections of future bankfull width (Figure 17). Specifically, the site provides the probability that a proposed culvert width will be inadequate (i.e., too narrow) at some point during its anticipated service life. The probabilities are calculated with the bootstrapped bankfull flow estimates following the same procedure outlined above: the areas of intersection between the drainage area and the grid cells are determined, the projected bankfull discharge at the culvert location is calculated as an area-weighted average of the bankfull discharges of the grid cells intersecting the drainage area, converting the bankfull flow estimates to bankfull width, then calculating the percent change for each time period. This is applied separately to each of the 1,000 bootstrapped bankfull flow estimates for each time period. As described in the previous section, the probability is then estimated by taking the fraction – among 1,000 percent change estimates – with a percent change in bankfull width that exceeds a user-specified culvert width. This process estimates the probability of an inadequate culvert width within each time period. We took this one step further by estimating the cumulative probability of an inadequate culvert width from 2020 to each future time period. This provides a time-

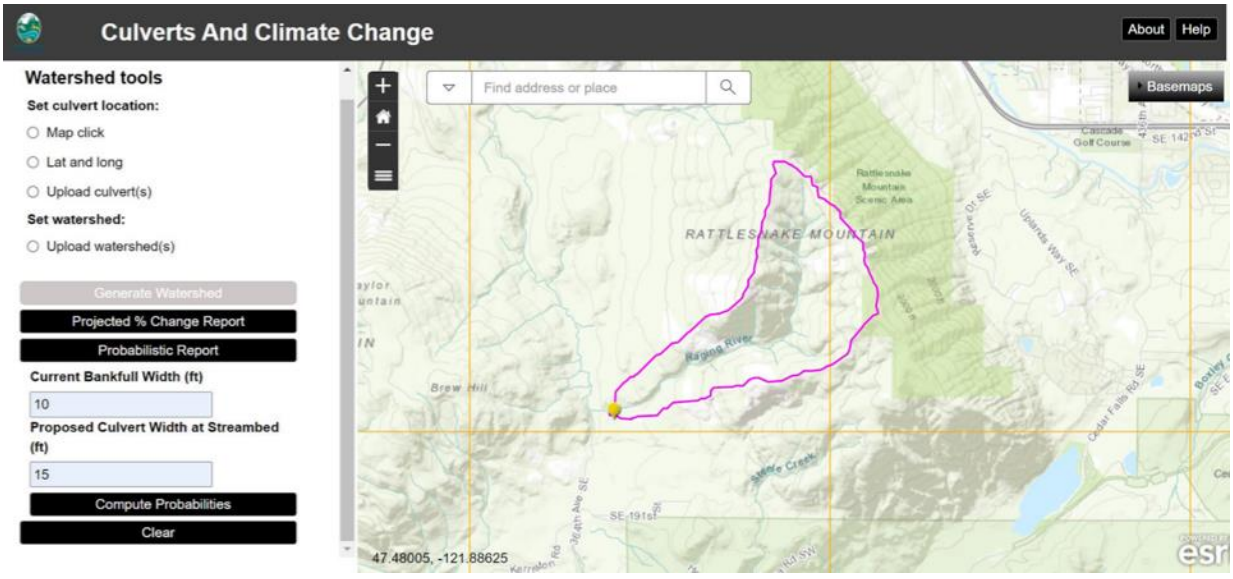

Figure 16. Example screenshot of the revised but yet to be released Culverts and Climate Change internet site.

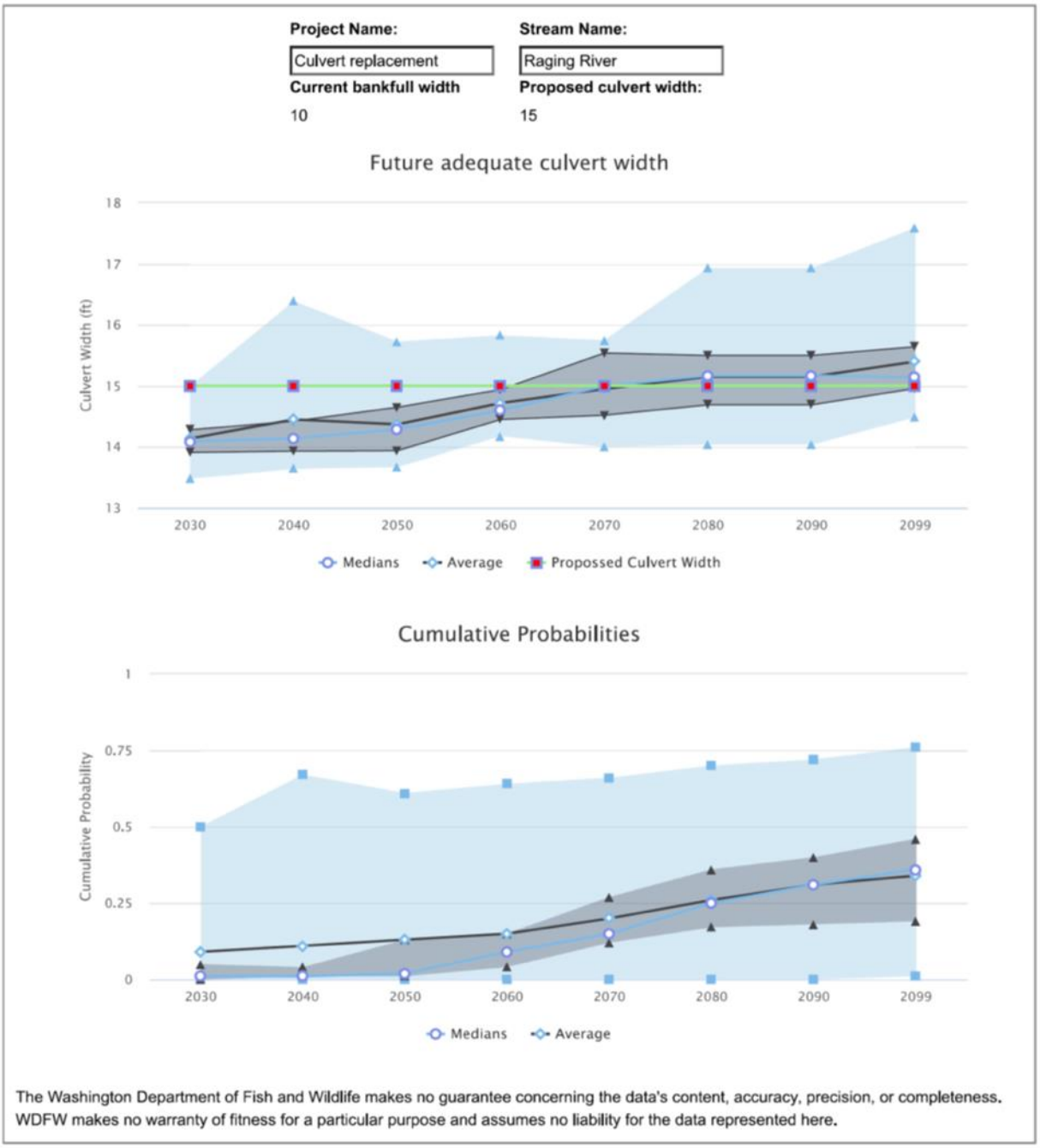

Figure 17. Example report providing cumulative probability of the proposed culvert width being too narrow over time (bottom) and adequate culvert widths over time (top) produced by Culverts and Climate Change internet site. On both graphs, gray envelop is inter-quartile range and light blue envelope is full range of values.

varying estimate of the probability that a proposed culvert size will meet the design requirement between now and each future decade.

In addition to the probabilistic output, the internet site also depicts the relationship between the proposed culvert width and the distribution of future adequate culvert widths (Figure 17). Both of these graphs – cumulative probability over time and adequate culvert widths over time – can be exported to a pdf. To obtain these two new outputs from the revised Culverts and Climate Change internet site, the user must enter the current bankfull width and a proposed culvert size (Figure 16). We envision that for some engineers, climate-adapted culvert design will be an iterative process in which the designer enters a set of proposed culvert widths and selects the culvert width that results in an acceptably low cumulative probability of the culvert being too narrow in the future.

Results

The historical simulations show the expected relationship between runoff, evaporation, and precipitation (Figure 18). Specifically, the average ratio of evaporation to precipitation ranges from ~0.1 for the windward slopes west of the Cascades to ~0.9 in the Columbia Plateau, with values ranging from 0.3-0.6 in the Puget Sound lowlands and middle elevations east of the Cascades. Potential evapotranspiration (PET) estimates show that the evaporative demand far outstrips precipitation in the Columbia Plateau, consistent with its high desert climate. PET is less than precipitation elsewhere, where evaporation is energy-limited. These results confirm that the model is accurately capturing the general features of the water balance.

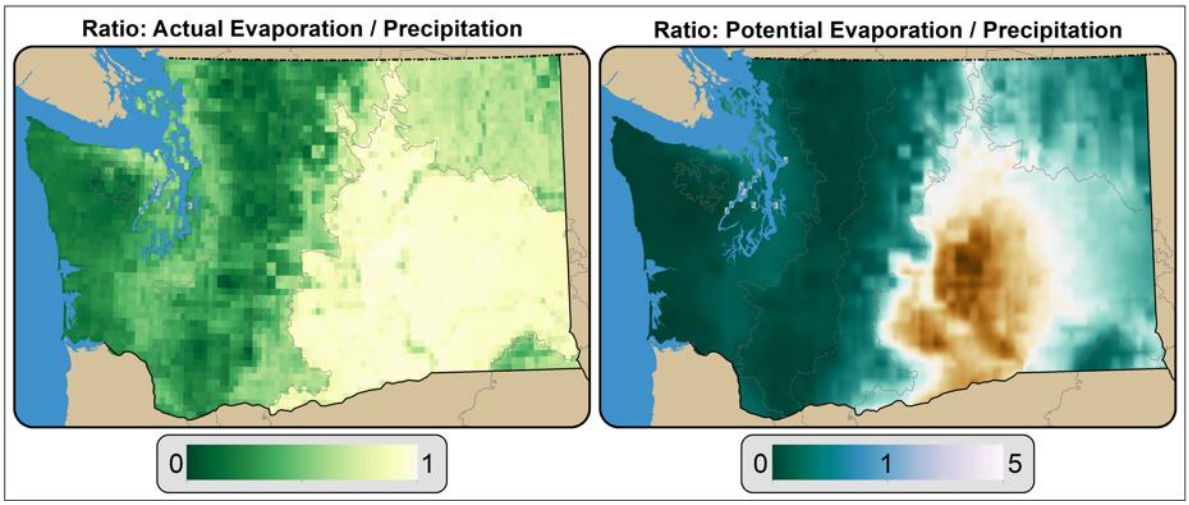

Figure 18. The water balance shows the expected pattern of variations across Washington State. Maps show the average ratio of actual evapotranspiration (AET) to precipitation (left) and potential evapotranspiration (PET) to precipitation (right). Given the dominant water balance in which precipitation is primarily partitioned among runoff and evapotranspiration, the left-hand map can also be subtracted from 1 to give the runoff ratio. The PET ratio map gives a measure of the imbalance between evaporative demand and precipitation.

Peak flows are the basis for culvert design and therefore the emphasis of this study. Figure 19 shows the average projected change in bankfull flow, which is the basis for calculating changes in bankfull width and the associated changes in stream simulation culvert size (Equations 1 and 2). Projected changes are shown for the 2080s (2070-2099, relative to 1970-2015), for the same high-end greenhouse gas scenario (RCP 8.5) used for all of the

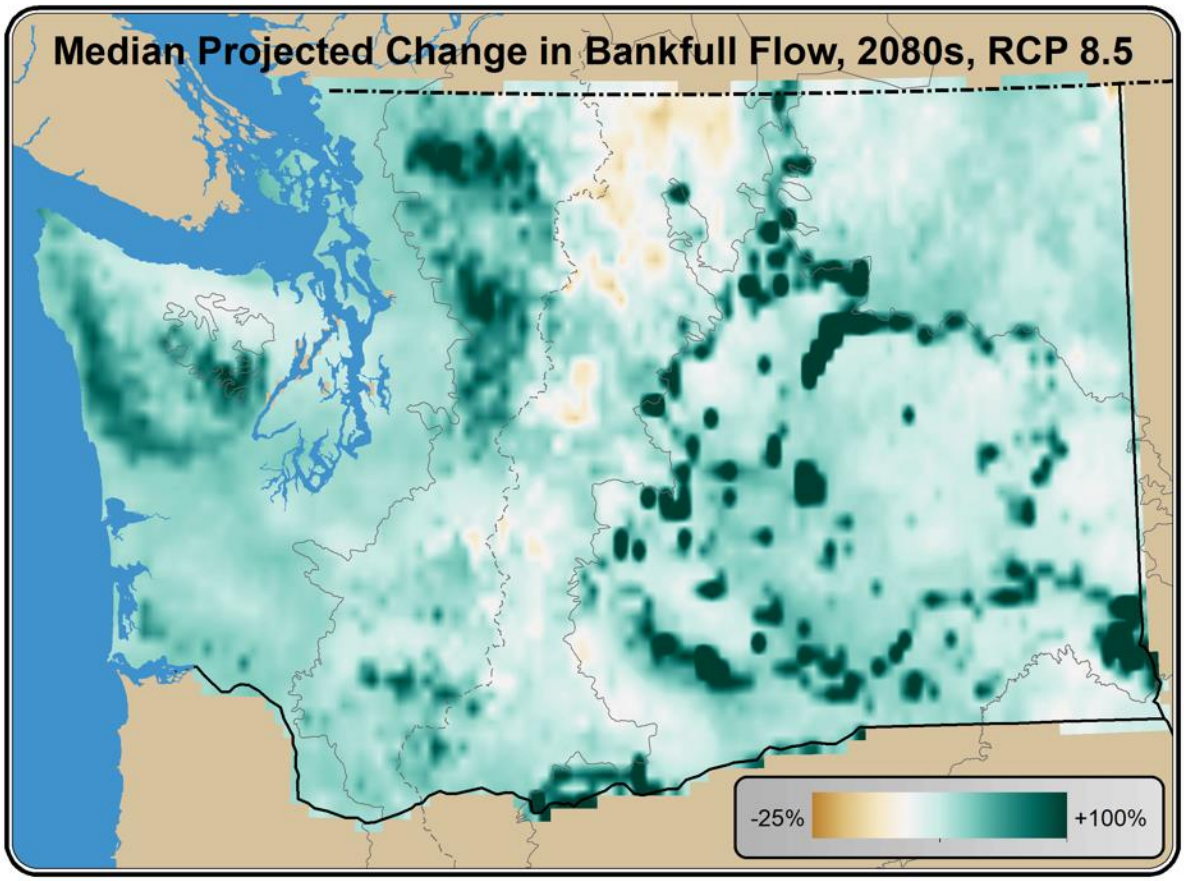

Figure 19. Change in bankfull flows. Projected changes are the median of all 12 model projections (RCP 8.5), expressed as a percent (%) change for the 2080s (2070-2099) relative to 1970-2015.

projections in this study. West of the Cascade crest, these show particularly large changes on the southwest slopes of the Olympics and in the northwestern Cascades, and the major volcanoes of the south Cascades (Mount Rainier, Helens, and Adams).

The model projects small decreases in bankfull flows for parts of the eastern Cascades. These correspond to areas where historical flood peaks occurred primarily during the spring peak in snowmelt. As snow accumulation decreases in the future, these locations shift to rain-driven flooding (Figure 20, left panel), but due to the lower intensity rainfall east of the crest, these floods tend to be smaller than the snow-driven floods of the past. This effect seems to be primarily isolated to the coldest portions of the east Cascades, likely corresponding to the areas with the greatest winter snow accumulation.

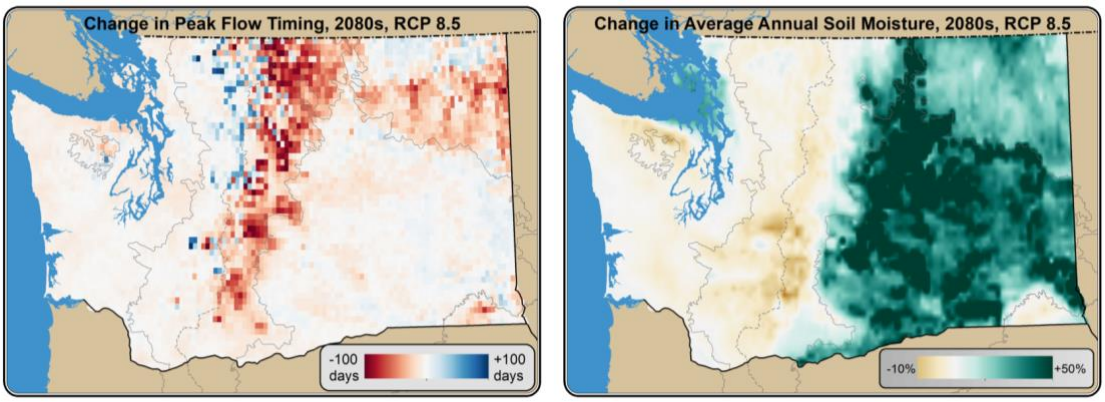

Figure 20. *Left panel:* Change in peak flow timing, an indicator of a shift from snowmelt to rain-driven peak flows. *Right panel:* Change in total soil moisture, an indicator of changes in the groundwater contributions to peak flows. Both show the change for the 2080s (2070-2099) relative to 1970-2015, for a high greenhouse gas scenario (RCP 8.5).

Another unexpected pattern in the new projections is the large increases projected for certain areas east of the Cascades. These are concentrated along the major rivers surrounding the Columbia Plateau (Columbia, Snake, Okanagan). First, it is worth noting that these changes are confined to very dry areas of the state, where historical flood peaks are very small and will continue to be small in the future, even if they are projected to increase substantially. The changes in these locations are a result of differences in the soil properties. These locations have a higher proportion of sand in their soils, making them more permeable. As a result, more precipitation infiltrates the soils (Figure 20, right panel). In the VIC model, this translates to greater soil water storage in the bottom soil layer, which is beyond the reach of roots – meaning that this extra water storage cannot be lost to evaporation. Instead, these areas with sandier soils have a higher relative contribution from groundwater to flood peaks than otherwise similar areas with less sandy soils. The models generally project higher precipitation for the Columbia Plateau in the future, meaning that this groundwater contribution to flood peaks increases in the future. Since historical flood peaks were already small, even a fairly small increase in soil water storage can lead to notable increases in bankfull flows.

Figure 21 shows the projected change in bankfull flows alongside the projected changes for

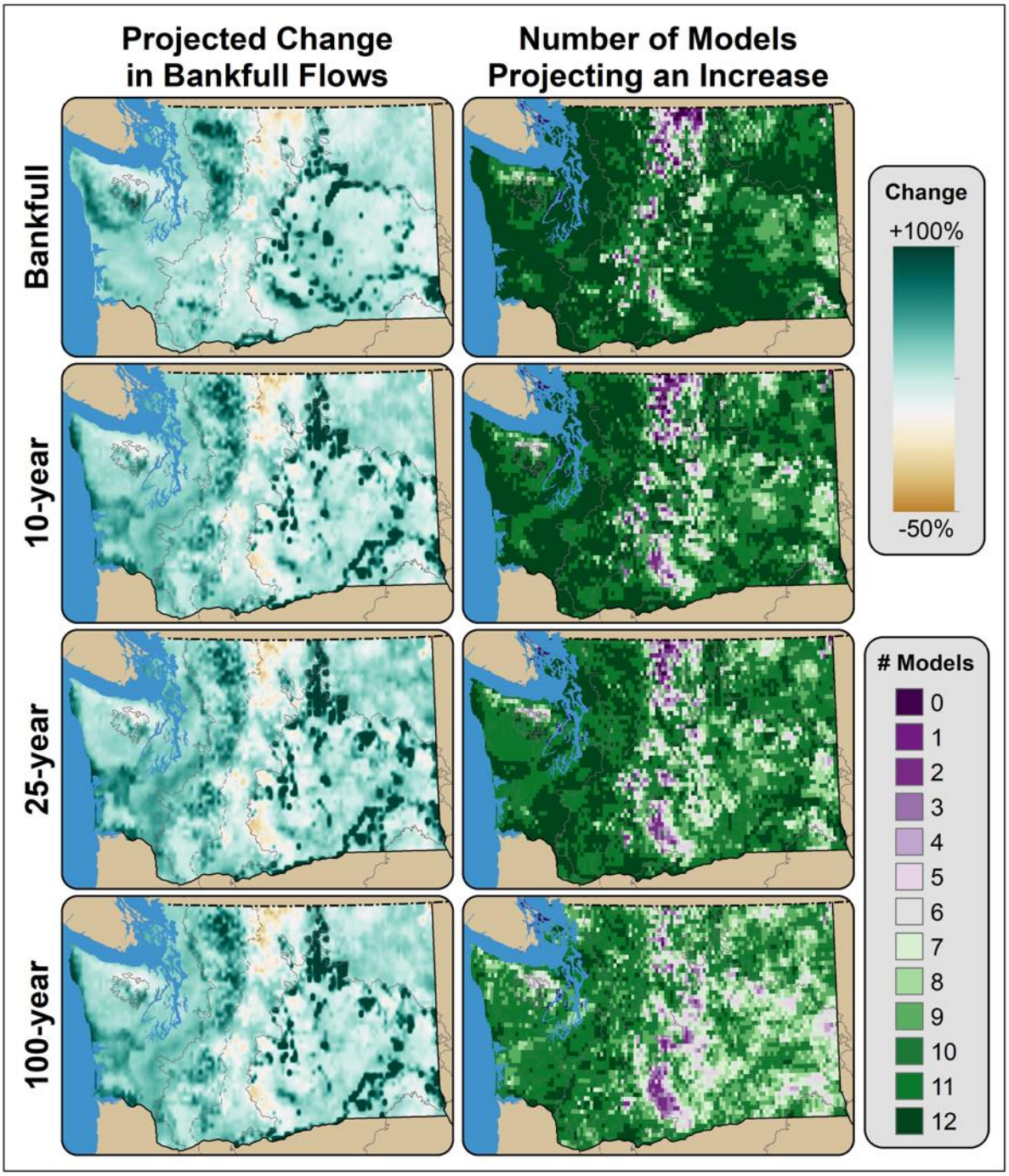

Figure 21. Average change (left) and number of models projecting an increase (right), for bankfull flows and the 10-, 25-, and 100-year peak flow events. Projected changes are the average of all 12 model projections (RCP 8.5), expressed as a percent (%) change for the 2080s (2070-2099) relative to 1970-2015.

the 10-, 25-, and 100-year peak flow events. As a measure of the uncertainty in the changes, the figure also includes maps showing the number of models that project an increase in each flow metric. These results show similar patterns of change across all peak flow metrics.

To illustrate the probabilistic approach, Figure 22 shows maps of the probability of a particular increase (10% through 40%), for each grid cell, by the 2080s. As described above, these provide the probability that a specific percent change will be reached between now and the 2080s. The current map is assessed in terms of bankfull flows, whereas culvert design is specified in terms of bankfull widths. Either can be assessed using the probabilistic approach.

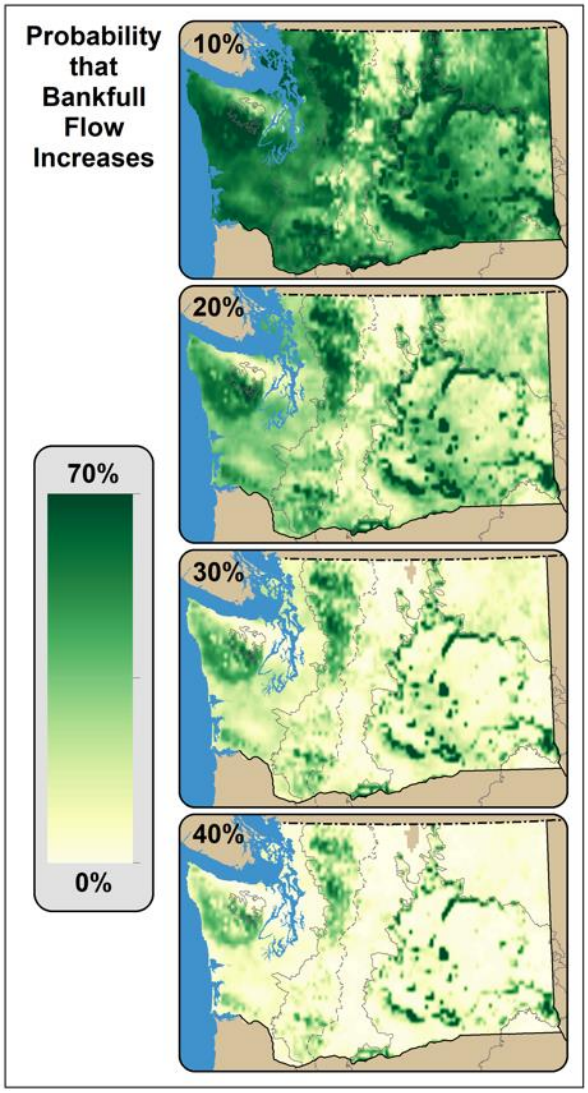

Figure 22. Probability that bankfull flows increase by 10% (top row), 20% (2nd row), 30% (3rd row), and 40% (bottom row) by the 2080s. All changes are assessed relative to 1970-2015, for the high-end RCP 8.5 scenario.

Finally, we compare our results with the results of our previous projections for changes in bankfull flows (Figure 23, Wilhere et al. 2016). West of the Cascades, these show the same overall pattern of change, likely due to the higher density of observations in this area and the fact that both historical and future peak flows are primarily driven by changes in heavy rainfall. Nonetheless, there are key differences between the projections west of the Cascades. In particular, the 2016 results tend to show the largest increases at upper elevations, whereas the new results show the largest increases on the southwest slopes of key topographic features. The latter is more consistent with the meteorology of the region,

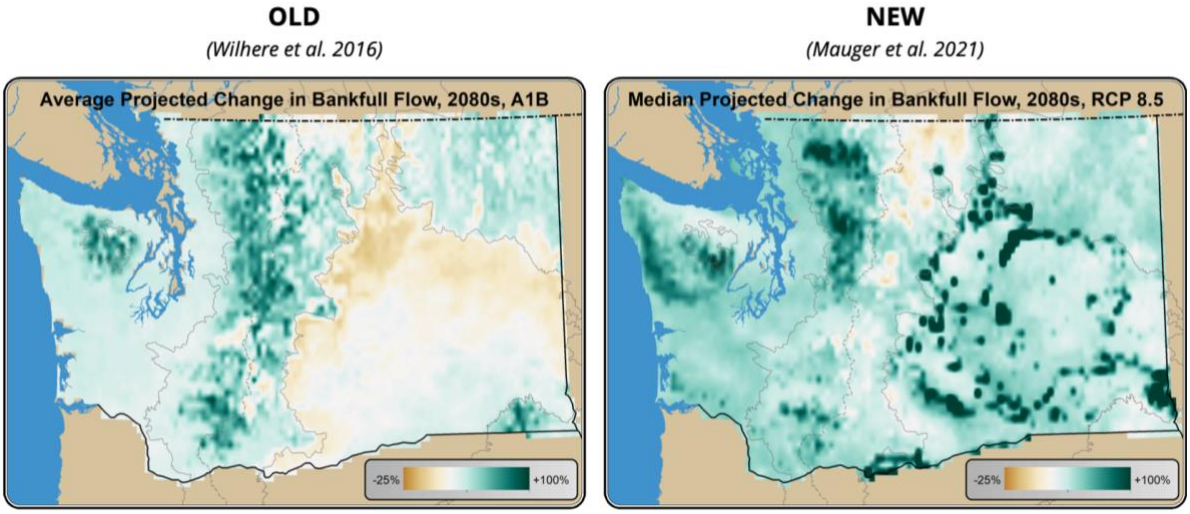

Figure 23. Comparing older bankfull flow projections (left, Wilhere et al. 2016), with the new projections that are described in the current study (same map as in Figures 18 and 19). Both show the change for the 2080s (2070-2099) relative to 1970-2015, for a high greenhouse gas scenario (RCP 8.5).

where the highest intensity precipitation occurs on the mid-elevation windward slopes. Similarly, the new projections clearly show the rain shadow effect in the lee of the Olympics and even other smaller topographic features in western Washington (e.g., the Willapa Hills on the southern Olympic Peninsula).

The biggest differences between the new and old results are east of the Cascade crest. The 2016 results showed much larger increases over the topography – including the eastern slopes of the Cascades, Okanagan mountains, and Blue Mountains in southeastern Washington – likely due to the same over-simplification in which the old projections showed systematic increases in precipitation at higher elevations. The new projections, in contrast, capture the stark differences in precipitation east and west of the Cascade mountains. Another major difference in the projections is the location of the projected decreases in bankfull flows. In both cases, the decreases can be traced back to a decline in snowpack, where areas that previously had snowmelt-driven peak flows, occurring in spring, switch to rain-driven peak flows in fall/winter. The 2016 results do not capture the projected decreases on the eastern slopes of the Cascades, likely because precipitation is overestimated for these locations.

Where the 2016 results do show decreases – around the perimeter of the Columbia Plateau – the same areas show increases in the new results. The 2016 results underestimated changes in heavy precipitation events, by assuming that they would change in tandem with monthly average precipitation. The new projections include the larger – and more accurate – changes that are projected for heavy rain events. Since these increase more in the new results, the change is large enough to offset the small decrease in peak flows due to declining snowmelt in the future.

Conclusions

There are two primary pathways for climate change to influence peak flows in Washington State: (1) decreasing snowpack and (2) higher intensity precipitation events. Snowpack declines generally lead to increased flooding by increasing the portion of the watershed that receives rain during winter storm events. This increase in the proportion of rainfall relative to snowfall relates directly to the volume of water supplied to streams and rivers during a flood event. In a few areas east of the Cascade crest, declining snowpack can instead lead to decreases in flood peaks if individual rain events are not particularly intense compared to the snowmelt-driven peaks of the past. Snowpack has already declined significantly over recent decades and is projected to continue declining throughout this century (Mote et al. 2018). This is a consequence of climate change that will be important over the near-term as many parts of the region transition from snow-influenced to fully rain-dominant. Heavy rain events are projected to become more intense, particularly in the second half of this century (Warner et al. 2015). As with the declines in winter snowpack, this translates directly into more water in streams during flood events. Changes in rainfall intensity will be more important later in the century; near-term changes are likely to be primarily a consequence of declining snowpack.

Overall, our results indicate that bankfull flows will increase substantially over most of the state, with some isolated areas experiencing decreases where snowmelt is currently the primary driver of peak flows on the eastern slopes of the Cascades. Our results show a high degree of agreement among all 12 climate models used in the projections. The hydrologic model calibration performs best west of the Cascades and in the mountainous areas east of the Cascade crest, whereas our validation results show that the model struggles to accurately represent the hydrology of the Columbia Plateau.

All projections are shared on our website and available via the updated internet tool, which allows users to view projections for specific locations of interest to them. Our probabilistic results allow users to assess the probability that a particular design size will meet the regulatory requirement over the culvert's lifetime.

Interpreting the results

Interpretation of these results, particularly given the focus on extreme events, can be challenging. Following are a few considerations to keep in mind when reviewing the results:

- Projected changes will always be governed by a combination of random variability and long-term trends due to climate change. We based our projections on 30-year time periods, since averaging over 30 years is likely to significantly reduce the effect of natural variability. Nonetheless, it is possible that multi-decadal variations in climate can obscure trends in some instances. We recommend considering multiple lines of evidence (e.g., multiple return intervals and durations) before concluding that a particular trend is to be expected.
- By definition, extreme events are rare. This makes it difficult to assess how rapidly they change. In particular, our use of 30-year periods limits the return intervals that can be reliably quantified. This is unlikely to be an issue for bankfull flows, which are based on the 1.2- to 1.5-year event and therefore well captured in a 30 year interval. In contrast, the 50-, 100-, and 500-year events can only be estimated by extrapolating from the GEV distribution. Even the 15-year event could be under-sampled, given that it would only occur twice, on average, in each 30-year time period. Our bootstrap approach should help reduce the effects of outliers. Nonetheless, we recommend focusing on the results for the more frequent events since these are likely to be most accurate.
- The WRF model used in this study has a spatial resolution of 12 km. While much better than the resolution afforded by GCMs, this is still coarse relative to some weather and topographic features. For example, thunderstorms are not resolved at a resolution of 12 km. Although in most locations thunderstorms are not an important driver of peak flows, they can be a defining feature of the hydrology for culverts that are located in areas with thunderstorm potential (e.g., high elevation Cascades, eastern slopes of the Cascades). In these areas, a different approach may be needed to estimate future flows.
- A limitation of complex hydrologic models such as VIC is that there are more parameters to tune than there are observations with which to constrain them. This means that it is possible for calibration to lead to "the right answer for the wrong reason". This is an especially challenging issue with climate change, since a model that performs well under current conditions may not be able to accurately capture changes in flow under future climate conditions. We have tested the model

calibration in multiple ways in order to avoid this pitfall, but cannot be sure that the issue does not remain.

- A further challenge in calibrating the model for the current study is that culverts often drain an area that is smaller than a single grid cell, yet individual grid cell calibration is not possible since long-term observations cannot be feasibly obtained for every grid cell in the domain. Instead, calibration must be applied "globally", where calibrated parameters are applied uniformly across regions based on shared characteristics. This inevitably leads to trade-offs where the model performs better for some locations than for others.
- The VIC model is not able to capture deep or confined groundwater. While important for low flows, groundwater is unlikely to be an important contributor to peak flows in most locations, with the possible exception of the driest parts of the state in and around the Columbia Plateau.
- In a recent study comparing evapotranspiration estimates, Milly and Dunne (2017) found that most hydrologic models dramatically overestimate future changes in evapotranspiration. This includes the Penman-Monteith method used in VIC. This is not likely to be an issue for peak flow simulations. However, this could have important implications for summer flows, and would be important to estimate correctly in any future study evaluating the implications of possible changes in land cover.
- The streamflow projections are based on current landcover conditions. Forestry practices and further urbanization could also significantly affect future flows, as could increases in the frequency and extent of wildfire due to climate change. Modifications to the land cover in VIC could be used to assess forest harvest or wildfire impacts in future modeling assessments. This was not evaluated in the current study.
- Our results concern changes in naturalized flows (i.e.: no reservoirs or water withdrawals). Although reservoir operations are unlikely to be relevant to culvert design, water withdrawals upstream of a culvert could be an important factor affecting design. Such effects are not included in the current study.
- This project has focused on quantifying the changes in peak flows that may affect the performance of culverts in the future. A complementary assessment is needed to evaluate (1) the "sensitivity" to these changes – how impacts scale with future

changes, and (2) the "adaptive capacity" – how much these changes can be mitigated by changes in land use and water management or salmonid life history characteristics. Work to better understand these complementary aspects of vulnerability would help clarify if, when, and where to focus efforts at managing climate change risks.

Future Work

The science of climate change will continue to evolve over time due to changes in greenhouse gas scenarios, global climate models, downscaling approaches, and the hydrologic modeling used to make localized streamflow projections. In addition, further refinements to the existing approach could result in improved model estimates of current and future conditions. Future work could also further refine the approaches used to develop meteorological forcings and tune the VIC model.

With specific regard to the methods used in the current study, there are a number of near-term improvements that can be made to improve on the accuracy of the results. They are as follows:

1. IMPROVED BIAS CORRECTION OF TEMPERATURE AND PRECIPITATION: In the current work, WRF hourly temperature and precipitation inputs were bias-corrected to match the average monthly spatial pattern (or "climatology") from PRISM. Although in general, previous work suggests that an approach similar to this – that blends dynamical and interpolated datasets – is likely the best strategy, insufficient time was taken to evaluate the model performance for different approaches to bias-correction. For instance, a different approach may be needed for each ecoregion, or possibly each watershed. Hydrologic modelers consistently find that the accuracy of the meteorological inputs is by far the most important factor affecting the accuracy of streamflow estimates. Future work should devote more time to ensuring that the meteorological inputs are sufficiently bias-corrected.
2. REVISIT SOIL AND VEGETATION CHARACTERISTICS: The current work used new soil and vegetation inputs, that weren't used in previous implementations of the VIC model over Washington State. Although unlikely to dramatically alter the results, results with these new inputs should be compared against results using the previous soil and vegetation characteristics, to better understand the implications of

this change. Given that some of the concerning results in the current study stem from an interplay between the meteorological inputs and the model soil properties, this evaluation should compare not just the average flows but the sensitivity of peak flows to variations in climate.

3. VALIDATE SNOW SIMULATIONS (NOT JUST STREAMFLOW): In the current work, the model was calibrated entirely based on streamflow simulations. This is just one constraint on model performance and does not ensure that the model is accurately representing important process that could contribute to streamflows. By first evaluating snow simulations from the model – via both point comparisons with SNOTEL stations and a qualitative evaluation of snow-covered area – the model can be further tested to ensure that the model configuration and meteorological inputs are not resulting in biased estimates of snowpack. This is particularly useful as a way of testing the meteorological inputs, lapse rate assumptions, and snow/rain thresholds. In future work we recommend validating the model's snow simulation before proceeding to subsequent phases of model adjustment and calibration.
4. IMPROVED HYDROLOGIC MODEL CALIBRATION: The current study tested 40 randomly-generated parameter sets, selecting the top-performing ones for use in developing model projections. Typically, hydrologic model calibration is performed using many more parameter sets (at least 500), in order to adequately explore the parameter space. Although we chose 40 to minimize computation time, our findings suggest that was not sufficient. Future work should more thoroughly explore the parameter space, possibly using a test watershed to refine methods before applying the same approach to all calibration sites. An automated calibration approach may be the best approach (e.g., the MOCOM-UA algorithm; Yapo et al., 1998).
5. SYSTEMATIC APPROACH TO GENERALIZING CALIBRATED PARAMETERS: The calibration sites do not cover the entire state. As a result, parameters need to be generalized to provide calibrated flow estimates for the entire state of Washington. In the current work, we identified optimal parameter sets based on a subjective analysis of NSE and NSE-log scores, primarily focusing on the median NSE-log score for each ecoregion. Future work could either (1) identify regions with similar hydrology, then coordinate the calibration among all sites within each region, or (2) calibrate all locations separately, by obtaining or estimating observed flows for all watersheds within the state (e.g.: Pan and Wood, 2013).

6. DEVELOP INDEPENDENT ESTIMATES OF STREAMFLOW CHANGE: Independent estimates of streamflow changes would bring greater confidence to the results. As above, these can be fairly simple to undertake or more complex. One possibility is to simply evaluate existing observations, to identify past trends and understand how flows relate to key climatic conditions (e.g., precipitation intensity). In some cases past events can be compared to climate projections to see how often such conditions may occur in the future. Another option is to evaluate projected changes in flow using the recently-developed Columbia River Climate Change dataset (Chegwidden et al., 2019). These results were not used in the current study because they are based on statistical downscaling. However, their calibration is likely superior to the current work, and they are currently available to analyze "off-the-shelf", so could be put to use with a minimal amount of additional effort. Future work should process this new dataset to compare its projections with those of Wilhere et al. (2016) and the analysis presented in this report.

Planning requires more than just better quantification of climate change impacts. Managers need to know which interventions are likely to be needed, which are most effective, and how the answers to these questions vary across the watershed. Once improved models have been developed and calibrated, some questions can be answered more easily. For example, the model presented in this study can be used to look at the implications of land cover change on streamflow.

The domain of the regional climate model used to develop these projections covers the entire Pacific Northwest, stretching from northern California to British Columbia and from the west coast through the Rocky Mountains of Montana and Wyoming. This means that the approach we used here could be evaluated for other states around the region, or even the nation as a whole. For example, several states and federal agencies have similar stream simulation standards for culvert design; projections could be evaluated to assess the associated future changes in culvert sizes beyond Washington State and the standards applied by WDFW.

Finally, culvert project proponents and designers have benefited from the migration of the Culverts and Climate Change site from WDFW's intranet to a publicly-accessible internet site. Based on user feedback we have received, we know that the current site has been used for culvert design. However, we do not how much it has been used or whether use of

the internet site has led to construction of a climate-adapted culvert. At present, climate-adapted culverts are voluntary in Washington State. As a result, culvert permit applications are not required to contain information about climate adaptation. WDFW is currently conducting a rule-making process for revising rules related to fish passage (Chapter 77.57 Revised Code of Washington), which will include revised rules for culverts. We anticipate that the revised rules will include stipulations pertaining to climate-adapted culverts.

In anticipation of revised rules pertaining to climate-adapted culverts, WDFW will subject both the current results and the updated internet tool to additional testing. If time and resources allow, WDFW will also reconvene a group of users (i.e., culvert project proponents and designers), at another workshop to obtain feedback on the revised internet site. We will also renew our outreach and education efforts pertaining to climate-adapted culverts that were curtailed by the COVID pandemic.

References

Bandaragoda, C., Hamlet, A. F., Istanbulluoglu, E. (2021). Hybrid methods for producing gridded meteorological forcings in mountain environments. *In review*.

Barnard, R.J., Johnson, J., Brooks, P., Bates, K.M., Heiner, B., Klavas, J.P., Ponder, D.C., Smith, P.D., Powers, P.D., 2013. Water Crossing Design Guidelines. Washington Department of Fish and Wildlife, Olympia, WA.

Byun, K., A.F. Hamlet, 2020: A risk-based analytical framework for quantifying non-stationary flood risks and establishing infrastructure design standards in a changing environment, Journal of Hydrology, 584, 125575, https://doi.org/10.1016/j.jhydrol.2020.124575

Cenderelli, D., K. Clarkin, R. Gubernick, and M. Weinhold. 2011. Stream simulation for aquatic organism passage at road-stream crossings. Transportation Research Record: Journal of the Transportation Research Board 2203:36-45.

Chegwidden, O. S., Nijssen, B., Rupp, D. E., Arnold, J. R., Clark, M. P., Hamman, J. J., ... & Xiao, M. (2019). How do modeling decisions affect the spread among hydrologic climate change projections? Exploring a large ensemble of simulations across a diversity of hydroclimates. Earth's Future, 7(6), 623-637.

Dulière, V., Zhang, Y., & Salathé Jr, E. P. (2011). Extreme Precipitation and Temperature over the US Pacific Northwest: A Comparison between Observations, Reanalysis Data, and Regional Models*. Journal of Climate, 24(7), 1950-1964.

Friedl, M. A., Sulla-Menashe, D., Tan, B., Schneider, A., Ramankutty, N., Sibley, A., and Huang, X. (2010). MODIS Collection 5 global land cover: Algorithm refinements and characterization of new datasets. Remote Sensing of Environment, 114, 168–182.

Fuster, B. ; Sánchez-Zapero, J. ; Camacho, F. ; García-Santos, V. ; Verger, A. ; Lacaze, R. ; Weiss, M. ; Baret, F. ; Smets, B. Quality Assessment of PROBA-V LAI, fAPAR and fCOVER Collection 300 m Products of Copernicus Global Land Service. Remote Sensing 2020, 12137, 1017. DOI 10.3390/rs12061017

(gNATSGO) Soil Survey Staff. Gridded National Soil Survey Geographic (gNATSGO) Database for Washington State. United States Department of Agriculture, Natural Resources

Conservation Service. Available online at https://nrcs.app.box.com/v/soils. Feb 10, 2020.

Hamlet, A. F., Elsner, M. M., Mauger, G. S., Lee, S. Y., Tohver, I., & Norheim, R. A. (2013). An overview of the Columbia Basin Climate Change Scenarios Project: Approach, methods, and summary of key results. Atmosphere-ocean, 51(4), 392-415.

Hamman, J. J., Nijssen, B., Bohn, T. J., Gergel, D. R., and Mao, Y. (2018). The Variable Infiltration Capacity model version 5 (VIC-5): infrastructure improvements for new applications and reproducibility, Geosci. Model Dev., 11, 3481-3496, https://doi.org/10.5194/gmd-11-3481-2018

Homer, Collin G., Dewitz, Jon A., Jin, Suming, Xian, George, Costello, C., Danielson, Patrick, Gass, L., Funk, M., Wickham, J., Stehman, S., Auch, Roger F., Riitters, K. H., Conterminous United States land cover change patterns 2001–2016 from the 2016 National Land Cover Database: ISPRS Journal of Photogrammetry and Remote Sensing, v. 162, p. 184–199, at https://doi.org/10.1016/j.isprsjprs.2020.02.019

Jin, S., Homer, C.G., Yang, L., Danielson, P., Dewitz, J., Li, C., Zhu, Z., Xian, G., and Howard, D. 2019, Overall methodology design for the United States National Land Cover Database 2016 products. Remote Sensing, 11(24); https://doi.org/10.3390/rs11242971

Jung, M., Reichstein, M., Ciais, P., Seneviratne, S. I., Sheffield, J., Goulden, M. L., ... & Zhang, K. (2010). Recent decline in the global land evapotranspiration trend due to limited moisture supply. Nature, 467(7318), 951-954. https://doi.org/10.1038/nature09396

Kandlikar, M., Risbey, J., Dessai, S., 2005. Representing and communicating deep uncertainty in climate change assessment. Comptes Rendus Geoscience 337, 443–455.

Knutti, R., Furrer, R., Tebaldi, C., Cermak, J., Meehl, G.A., 2010. Challenges in combining projections from multiple climate models. Journal of Climate 23, 2739–2758.

Liang, X., D. P. Lettenmaier, E. F. Wood, and S. J. Burges (1994), A simple hydrologically based model of land surface water and energy fluxes for general circulation models, J. Geophys. Res., 99(D7), 14415–14428, doi:10.1029/94JD00483.

NASA Shuttle Radar Topography Mission (SRTM) (2013). Shuttle Radar Topography Mission (SRTM) Global. Distributed by OpenTopography. https://doi.org/10.5069/G9445JDF Accessed: 2021-03-04

NMFS (National Marine Fisheries Service), 2022. Improving Resilience into the Analysis and Design of Fish Passage Facilities. NOAA Fisheries West Coast Regional Office, 1201 Northeast Lloyd, Portland, Oregon 97232.

Pan, M., & Wood, E. F. (2013). Inverse streamflow routing. Hydrology and Earth System Sciences, 17(11), 4577–4588. https://doi.org/ 10.5194/hess-17-4577-2013

PRISM Climate Group, Oregon State University, http://prism.oregonstate.edu, created 4 Feb 2004.

Stephenson, D.B., Collins, M., Rougier, J.C., Chandler, R.E., 2012. Statistical problems in the probabilistic prediction of climate change. Environmetrics 23, 364–372.

Tebaldi, C., Arblaster, J.M., Knutti, R., 2011. Mapping model agreement on future climate projections. Geophysical Research Letters 38, L23701.

Wilhere, G.F., J.B. Atha, T. Quinn, I. Tohver, and L. Helbrecht. 2017. Incorporating climate change into culvert design in Washington State, USA. Ecological Engineering 104, 67-79.

Yang, Limin, Jin, Suming, Danielson, Patrick, Homer, Collin G., Gass, L., Bender, S.M., Case, Adam, Costello, C., Dewitz, Jon A., Fry, Joyce A., Funk, M., Granneman, Brian J., Liknes, G.C., Rigge, Matthew B., Xian, George, A new generation of the United States National Land Cover Database—Requirements, research priorities, design, and implementation strategies: ISPRS Journal of Photogrammetry and Remote Sensing, v. 146, p. 108–123, at https://doi.org/10.1016/j.isprsjprs.2018.09.006

Zhang, Y., Dulière, V., Mote, P. W., & Salathé Jr, E. P. (2009). Evaluation of WRF and HadRM Mesoscale Climate Simulations over the US Pacific Northwest*. Journal of Climate, 22(20), 5511-5526.

Appendix A: Weather Stations used in WRF Evaluation

Tables listing all weather stations used in the evaluation of the WRF model.

Table A1. Ag Weather Network stations used in the WRF model evaluation

ID	Name	Lat./Lon.	Elv (m)	Years
100011	08CF15	46.58440N / 119.79750W	333	2019-2019
100140	100Circles	45.93430N / 119.80540W	152	2000-2019
100012	10SB04	45.94520N / 119.60880W	149	2019-2019
100013	10SB16	46.20330N / 119.30750W	269	2019-2019
300219	Addy	48.31760N / 117.83000W	520	2015-2019
310112	Ahtanum	46.55150N / 120.70670W	505	1998-2019
300031	Alder.Rdg	45.84740N / 119.89110W	210	2016-2019
310107	Alderdale	45.88520N / 119.88840W	187	2005-2019
330150	Almira	47.86680N / 118.89440W	808	2008-2019
300032	Anatone	46.19900N / 117.11300W	945	2008-2019
330169	Arlington	48.20160N / 122.22620W	10	2017-2019
331106	Arrowhead	48.05880N / 119.54970W	348	2005-2019
100010	Avalon	45.49760N / 121.58200W	601	2019-2019
300218	Azwell	47.93030N / 119.88000W	247	2015-2019
300027	Badger.Cyn	46.17920N / 119.27650W	201	2008-2019
300116	Basin.City	46.64510N / 119.16450W	248	1989-2019
100005	BearWallow	45.60900N / 121.56340W	297	2019-2019
100114	Benton.E	46.27570N / 119.45450W	208	1995-2019
100161	Benton.W	46.30180N / 119.56760W	283	2006-2019
100172	Big.Flat	46.36140N / 118.79640W	251	2006-2019
330037	Boyd.Dist	47.88510N / 120.07180W	610	2008-2019
330174	Brays.Land	47.75010N / 120.15540W	405	2006-2019
330171	Brewster.N	48.13270N / 119.74740W	374	2006-2019
330074	Brewster.S	48.06490N / 119.85790W	240	1994-2019
330043	Broadview	46.96610N / 120.50180W	455	2008-2019
310138	Buena	46.43700N / 120.29500W	269	1989-2019
110023	Canoe.Rdg	45.88220N / 119.75620W	275	2008-2019
100059	Carlson	46.14310N / 119.46100W	455	1989-2019
330168	Cashmere.N	47.51030N / 120.43150W	266	2006-2019
100008	Cemetery	45.57190N / 121.17650W	212	2019-2019
360001	Chehalis	46.67760N / 122.98590W	54	2016-2019
330035	Chelan.S	47.83670N / 120.08780W	383	2008-2019
330100	Chief.Joe	48.03060N / 119.64320W	495	2009-2019
300220	Chimacum	48.01090N / 122.77460W	50	2015-2019
300068	Chucker	45.97300N / 119.07890W	285	2009-2019
100037	Coffin	46.04050N / 119.30870W	371	1992-2019
300133	College.Pl	46.02750N / 118.39980W	225	1992-2019
300046	Connell.N	46.71460N / 118.90940W	341	2008-2019
810105	Corvallis	44.56640N / 123.23870W	64	2008-2019
330164	Coupeville	48.19950N / 122.68760W	24	2000-2019
310137	Cowiche	46.66390N / 120.70410W	497	1989-2019
300401	Craigmont	46.21930N / 116.41940W	1111	2016-2019

ID	Name	Lat./Lon.	Elv (m)	Years
330105	Crane	48.06580N / 119.79770W	518	2009-2019
309001	Curlew	48.85780N / 118.60850W	573	2017-2019
100000	Dallesport	45.63040N / 121.13240W	67	2019-2019
330029	Davenport	47.65660N / 118.13210W	752	2008-2019
300208	Dayton.NE	46.38270N / 117.87140W	700	2014-2019
300216	Dayton.NW	46.39410N / 118.05400W	634	2015-2019
330030	DesertAire	46.70930N / 119.91730W	185	2008-2019
100002	Dog.River	45.60310N / 121.50960W	344	2019-2019
100134	Eby	46.06670N / 119.07710W	463	1989-2019
330145	Ellisforde	48.79290N / 119.39680W	268	1999-2019
330040	Ephrata	47.17980N / 119.64030W	373	2007-2019
330125	Fairfield	47.41530N / 117.25570W	753	2008-2019
100113	Finley	46.13950N / 119.05930W	151	1992-2019
330021	Fir.Island	48.35650N / 122.42190W	0	2008-2019
100069	FishHook	46.29400N / 118.74110W	235	1992-2019
100067	Fourmile	45.98850N / 119.32290W	220	1993-2019
330023	Frenchman	47.01550N / 119.86920W	383	2008-2019
300206	Garfield.E	46.99750N / 117.05590W	849	2013-2019
330033	George	47.08980N / 119.99190W	426	2008-2019
310111	Gleed	46.69690N / 120.61550W	578	1994-2019
100139	Gramling	46.12440N / 119.21910W	408	1989-2019
300093	Grandview	46.26810N / 119.84660W	296	2012-2019
300209	Granger	46.38390N / 120.19100W	262	2014-2019
300213	Grayland	46.78720N / 124.07940W	6	2014-2019
300048	Green.Blff	47.81470N / 117.29940W	727	2009-2019
110029	Hamilton	46.25060N / 119.73910W	252	2002-2019
300202	Harrington	47.38710N / 118.29430W	661	2013-2019
300205	Hartline	47.64120N / 119.14920W	561	2013-2019
300132	Hatton	46.79310N / 118.85920W	393	2008-2019
100129	Horrigan	46.07740N / 119.76900W	289	1989-2019
100064	Horse.Hvn	46.04900N / 119.41320W	366	1992-2019
300034	Huntsville	46.30630N / 118.11520W	592	2009-2019
310029	Husum	45.86280N / 121.48760W	404	2015-2019
300079	Juniper	46.37970N / 119.00590W	212	2008-2019
100071	K2H	46.28700N / 118.64270W	341	1992-2019
310027	Konnowac	46.47100N / 120.37930W	265	2008-2019
300201	LaCrosse	46.85590N / 117.84930W	453	2013-2019
300214	Langley	48.00110N / 122.43280W	51	2014-2019
330024	Lawrence	48.88370N / 122.32140W	45	2008-2019
300028	Lind	47.00210N / 118.56580W	491	2008-2019
344108	Long.Beach	46.36880N / 124.03280W	3	2005-2019
330144	Loomis.Grd	48.77750N / 119.42790W	360	2005-2019
330158	Loomis.Val	48.81530N / 119.52070W	433	2006-2019
330063	Lynden	48.93560N / 122.51410W	21	2002-2019
310089	Mabton.E	46.19920N / 119.93000W	210	2008-2019
330028	Mae	47.06800N / 119.49230W	372	2008-2019
330167	Malaga	47.36490N / 120.23870W	294	2006-2019
330173	Malott	48.30470N / 119.68380W	405	2006-2019
330047	Mansfield	47.91700N / 119.78140W	844	2016-2019

ID	Name	Lat./Lon.	Elv (m)	Years
310025	Maryhill	45.67270N / 120.87320W	207	2008-2019
330121	Mattawa.E	46.70110N / 119.79960W	259	1989-2019
300117	McClure	46.37620N / 119.72430W	739	1989-2019
310077	McKinley	46.00670N / 119.91680W	329	2002-2019
100031	McNary	45.96900N / 119.25760W	230	1992-2019
300118	McWhorter	46.31680N / 119.61730W	427	1989-2019
300047	Mesa.SE	46.53180N / 119.00250W	233	2008-2019
100007	Mill.Creek	45.59330N / 121.22690W	207	2019-2019
310022	Montesano	46.97940N / 123.49470W	8	2008-2019
100006	Morgan	45.55220N / 121.19250W	365	2019-2019
330127	Moses.Lake	47.00450N / 119.23820W	340	1989-2019
310024	Moxee.E	46.55010N / 120.30220W	400	2008-2019
310143	Moxee.SE	46.54140N / 120.34560W	342	1989-2019
330101	Mt.Vernon	48.43850N / 122.38570W	7	1993-2019
310126	Naches	46.70440N / 120.65870W	417	2005-2019
330061	Nooksack	48.96680N / 122.30760W	25	2002-2019
330151	Olympia.E	46.95050N / 122.83530W	61	2010-2019
330078	Orondo	47.56650N / 120.24550W	271	2008-2019
330146	Oroville.E	48.97960N / 119.41340W	345	2005-2019
300122	Othello	46.79270N / 119.04130W	360	1989-2019
310135	Outlook	46.42250N / 120.13140W	390	1998-2019
310132	Parker	46.51720N / 120.47910W	287	1989-2019
100147	Pasco	46.25290N / 119.12740W	123	1995-2019
100025	Pasco.NW	46.38190N / 119.24560W	253	2008-2019
100062	Paterson.E	45.93910N / 119.48770W	129	1990-2019
300026	Paterson.W	45.93700N / 119.66260W	180	2008-2019
300203	Peshastin	47.55960N / 120.59250W	328	2013-2019
300210	PhinnyHill	45.90030N / 119.90180W	197	2014-2019
100066	Plymouth	45.96560N / 119.45660W	183	1993-2019
330104	Pogue.Flat	48.43540N / 119.52770W	385	2004-2019
310142	Pomona	46.69070N / 120.47250W	380	1989-2019
355001	Poulsbo.S	47.65640N / 122.64790W	37	2013-2019
300222	Prescott.N	46.33770N / 118.31540W	587	2015-2019
300033	Prosser	46.25700N / 119.74040W	265	1989-2019
300152	Pullman NE	46.77930N / 117.08540W	796	2011-2019
300029	Pullman.S	46.69640N / 117.14820W	760	2008-2019
310102	Puyallup	47.19300N / 122.32720W	10	1995-2019
330073	Quincy	47.22550N / 119.95680W	453	1989-2019
330022	Radar.Hill	46.71870N / 119.23820W	329	2008-2019
300253	Red.Mtn.N	46.29920N / 119.44230W	349	2015-2019
300254	Red.Mtn.S	46.27830N / 119.42090W	229	2016-2019
100148	Richland.N	46.33120N / 119.27020W	116	1995-2019
300021	Ringold	46.48400N / 119.17740W	267	2007-2019
300030	Ritzville	47.14140N / 118.47270W	553	2008-2019
310023	Roosevelt	45.73530N / 120.24390W	122	2008-2019
330041	RoyalCty.E	46.91520N / 119.51080W	341	2008-2019
320098	RoyalCty.W	46.97170N / 119.83460W	466	2008-2019
330099	RoyalSlope	46.94750N / 119.32090W	411	2009-2019
300045	Roza	46.29190N / 119.73310W	360	1989-2019

ID	Name	Lat./Lon.	Elv (m)	Years
330159	Sakuma	48.49740N / 122.37850W	9	2006-2019
330092	Seattle	47.65700N / 122.28910W	9	2011-2019
330039	Sequim	48.08670N / 123.05900W	30	2008-2019
810405	Silverton	45.03890N / 122.77690W	60	2008-2019
300023	Smith.Cyn	46.27610N / 118.98870W	157	2008-2019
310121	Snipes.Mtn	46.30970N / 120.07490W	381	2014-2019
330162	Snohomish	47.90270N / 122.11470W	0	2006-2019
131034	St.Andrews	47.64810N / 119.42050W	725	2008-2019
300043	St.John	47.07930N / 117.58900W	674	2008-2019
810305	St.Paul	45.13840N / 122.94850W	46	2008-2019
300207	Stevenson	45.68430N / 121.89850W	30	2013-2019
330115	Sunrise	47.30860N / 120.06850W	267	2008-2019
310136	Sunside.N	46.38560N / 119.99690W	329	1989-2019
310139	Sunside.NE	46.35680N / 119.90960W	338	2016-2019
310120	Sunside.S	46.28320N / 120.00940W	207	1993-2019
330025	Ten Mile	48.86610N / 122.47620W	20	2008-2019
330036	Thorp	47.07560N / 120.69340W	539	2008-2019
344109	Tokeland	46.70620N / 123.96730W	3	2010-2019
330157	Tonasket.S	48.68060N / 119.46090W	356	2006-2019
310031	Toppenish	46.37170N / 120.39290W	239	2008-2019
100128	Touchet	46.01920N / 118.67820W	168	1989-2019
100039	TripleS	46.21360N / 119.50080W	454	2001-2019
330153	Tumwater	46.94980N / 122.96390W	58	2011-2019
310032	Underwood	45.74120N / 121.56080W	396	2008-2019
310026	Vancouver	45.67770N / 122.65130W	71	2008-2019
300212	Vantage	46.82220N / 119.94270W	162	2014-2019
330044	Wahluke	46.76630N / 119.82000W	361	2008-2019
300130	WallaWalla	46.07760N / 118.27450W	359	1992-2019
300038	Wallula.S	46.07590N / 118.90750W	117	2008-2019
300215	Wallula.SW	45.97660N / 119.03160W	168	2015-2019
100004	Wamic.N	45.17660N / 121.29040W	599	2019-2019
100003	Wamic.S	45.17180N / 121.28920W	632	2019-2019
310131	Wapato	46.44110N / 120.52780W	256	1989-2019
330042	Warden.SW	46.93380N / 119.11920W	378	2008-2019
300143	Washtucna	46.78070N / 118.51530W	452	2015-2019
330046	Waterville	47.72140N / 120.07190W	945	2015-2019
300070	Welland	46.21740N / 118.73320W	291	1992-2019
330166	Wenatch.E	47.39960N / 120.19570W	384	2006-2019
330165	Wenatch.S	47.36680N / 120.30520W	707	2006-2019
330141	Wenatch.W	47.43950N / 120.34920W	241	1993-2019
330027	Wheeler	47.14490N / 119.06670W	442	2008-2019
100065	Wheelhouse	46.02540N / 119.52760W	269	1992-2019
100125	Whitcomb	45.86050N / 119.76440W	91	2007-2019
100001	Willis	45.66050N / 121.50970W	190	2019-2019
810205	Woodburn	45.12000N / 122.83730W	46	2008-2019
330026	Woodinvill	47.74840N / 122.15420W	14	2008-2019

Table A2. Global Historical Climate Network Dataset (GHCND) stations used in the WRF model evaluation. Stations that are bolded were also obtained from the SNOTEL dataset.

ID	Name	Lat. / Lon.	Elv. (m)	Years
USR0000BC83	83-MONUMENT-WASHINGTON	49.00170N / 120.64750W	1979	1985-2014
USC00450013	ABERDEEN-20NNE	47.26140N / 123.71470W	133	1927-2004
USC00450008	ABERDEEN-HCN	46.96580N / 123.82920W	3	1891-2019
USR0000WALD	ALDER-RIDGE-WASHINGTON	46.27330N / 117.49500W	1372	1985-2019
USC00450176	ANACORTES	48.51190N / 122.61360W	6	1892-2016
USC00450217	APPLETON	45.80920N / 121.28110W	712	1959-2006
USC00450257	ARLINGTON	48.20060N / 122.12810W	31	1922-2019
USC00450294	ASOTIN-14-SW	46.20390N / 117.24720W	1037	1976-2019
USC00450456	BARING	47.77220N / 121.48190W	235	1970-2019
USC00450482	BATTLE-GROUND	45.77170N / 122.52860W	87	1928-2019
USC00450587	BELLINGHAM-3-SSW-HCN	48.71780N / 122.51140W	5	1985-2019
USW00024217	BELLINGHAM-INTL-AP	48.79390N / 122.53720W	45	1949-2019
USC00450668	BICKLETON	45.99810N / 120.30060W	919	1927-2018
USC00450729	BLAINE-HCN	48.97750N / 122.79280W	18	1893-2019
USS0020B02S	Blewett-Pass	47.35000N / 120.68000W	1292	1980-2019
USC00450844	BOUNDARY-DAM	48.99470N / 117.35440W	560	1965-2019
USC00450872	BREMERTON	47.56890N / 122.68280W	34	1899-2019
USC00450945	BUCKLEY-1-NE-HCN	47.16940N / 122.00360W	209	1913-2012
USS0021C38S	Bumping-Ridge	46.81000N / 121.33000W	1405	1978-2019
USS0017A01S	Bunchgrass-Mdw	48.69000N / 117.18000W	1524	1980-2019
USR0000WCA4	CAMP-4-WASHINGTON	48.01810N / 120.23420W	1097	1985-2019
USR0000WCAN	CANYON-CREEK-WASHINGTON	45.91670N / 122.16670W	762	1985-2019
USC00451160	CARSON-FISH-HATCHERY	45.86780N / 121.97330W	346	1977-2019
USC00451205	CATHLAMET-6NE	46.22530N / 123.32890W	55	1959-2015
USC00451233	CEDAR-LAKE-HCN	47.41440N / 121.75610W	476	1898-2019
USC00451276	CENTRALIA-HCN	46.72000N / 122.95280W	56	1893-2019
USC00451350	CHELAN	47.83440N / 120.00060W	364	1890-2019
USC00451395	CHEWELAH	48.27330N / 117.74080W	509	1925-2019
USC00451400	CHIEF-JOSEPH-DAM	47.99670N / 119.64830W	254	1949-2019
USC00451414	CHIMACUM-4-S	47.95220N / 122.79080W	43	1926-2019
USC00451504	CLE-ELUM-HCN	47.18890N / 120.91310W	579	1899-2019
USC00451484	CLEARBROOK-HCN	48.96720N / 122.32920W	20	1903-2019
USC00451496	CLEARWATER	47.57110N / 124.29220W	24	1895-2017
USC00451586	COLFAX	46.88330N / 117.35000W	604	1892-2013
USC00451630	COLVILLE-HCN	48.56780N / 117.93560W	474	1899-2019
USC00451666	CONCONULLY-HCN	48.55580N / 119.74920W	704	1894-2015
USC00451679	CONCRETE-PPL-FISH-STN	48.53970N / 121.74220W	59	1905-2019
USC00451690	CONNELL-1-W	46.66440N / 118.88280W	311	1960-2003
USC00451691	CONNELL-12-SE	46.50860N / 118.78780W	329	1951-2017
USS0021B13S	Corral-Pass	47.02000N / 121.46000W	1768	1980-2019
USC00451760	COUGAR-6-E	46.06250N / 122.20440W	201	1953-2019
USS0021B42S	Cougar-Mountain	47.28000N / 121.67000W	975	1980-2019
USR0000WCOU	COUGAR-MOUNTAIN-WASHINGTON	47.91670N / 123.11720W	914	1985-2019
USC00451767	COULEE-DAM-1-SW	47.95440N / 118.99970W	524	1934-2019
USC00451783	COUPEVILLE-1-S	48.20720N / 122.69140W	15	1895-2019
USC00451939	CUSHMAN-POWERHOUSE-#2-HCN	47.37060N / 123.16000W	6	1973-2019
USC00451992	DARRINGTON-RS	48.26000N / 121.60360W	168	1911-2019

ID	Name	Lat. / Lon.	Elv. (m)	Years
USC00452007	DAVENPORT-HCN	47.65750N / 118.16140W	722	1893-2019
USC00452030	DAYTON-1-WSW-HCN	46.31530N / 118.00220W	475	1893-2019
USR0000WDEE	DEER-MOUNTAIN-WASHINGTON	48.80190N / 117.61030W	1006	1985-2019
USW00094119	DEER-PARK-AP	47.97420N / 117.42830W	668	1998-2019
USC00452157	DIABLO-DAM	48.71420N / 121.14310W	272	1914-2019
USC00452220	DOTY-3-E	46.62970N / 123.21060W	79	1978-2007
USR0000WDIR	DOUGLAS-INGRAM-RIDGE-WASHINGTO	48.11560N / 120.10310W	1085	1985-2019
USR0000WDOU	DOUGLAS-WASHINGTON	47.62000N / 119.89830W	771	1990-2019
USR0000WDRY	DRY-CREEK-WASHINGTON	47.73330N / 120.53330W	1061	1987-2019
USC00452253	DRYAD	46.63640N / 123.25970W	92	1963-2019
USC00452384	EASTON	47.24220N / 121.18690W	661	1905-2019
USR0000WELR	ELK-ROCK-WASHINGTON	46.35220N / 122.60580W	762	1985-2019
USW00024220	ELLENSBURG-BOWERS-FLD	47.03390N / 120.53030W	538	1940-2019
USC00452505	ELLENSBURG-HCN	46.96920N / 120.54000W	451	1893-2019
USC00452531	ELMA	47.00920N / 123.40080W	21	1896-2019
USC00452542	ELTOPIA-8-WSW	46.39920N / 119.15610W	213	1974-2007
USC00452548	ELWHA-RS	48.01640N / 123.59060W	110	1942-2018
USC00452563	ENTIAT-FISH-HATCHERY	47.69830N / 120.32280W	313	1989-2019
USW00024141	EPHRATA-MUNI-AP-72790	47.30780N / 119.51530W	382	1949-2019
USC00452675	EVERETT-HCN	47.97530N / 122.19500W	18	1894-2019
USW00024222	EVERETT-SNOHOMISH-AP	47.90780N / 122.28030W	185	1948-2019
USR0000WFIN	FINNEY-CREEK-WASHINGTON	48.40280N / 121.79030W	579	1985-2019
USR0000WFIR	FIRST-BUTTE-WASHINGTON	48.61720N / 120.10750W	1676	1985-2019
USS0021B04S	Fish-Lake	47.54000N / 121.09000W	1046	1980-2019
USC00452914	FORKS-1-E-HCN	47.95580N / 124.35390W	107	1907-2019
USW00094276	FRIDAY-HARBOR-AP	48.52220N / 123.02310W	33	1998-2019
USC00453177	GLENOMA	46.51860N / 122.13830W	256	1966-2004
USC00453184	GLENWOOD-#2	46.00890N / 121.26330W	580	1979-2012
USR0000WGOH	GOLD-HILL-WASHINGTON	48.20000N / 121.50000W	1036	1990-2019
USC00453222	GOLDENDALE-HCN	45.80810N / 120.84280W	500	1905-2019
USC00453320	GRAYLAND	46.80080N / 124.08640W	3	1948-2013
USC00453333	GRAYS-RVR-HATCHERY	46.38720N / 123.56030W	31	1962-2019
USS0021C10S	Green-Lake	46.55000N / 121.17000W	1804	1982-2019
USS0020B11S	Grouse-Camp	47.28000N / 120.49000W	1643	1980-2019
USR0000WHAG	HAGER-CREEK-WASHINGTON	46.56670N / 121.63060W	1097	1985-2019
USC00453515	HARRINGTON	47.48280N / 118.25190W	658	1961-2019
USC00453529	HARTLINE	47.68920N / 119.10640W	581	1927-2019
USS0020A05S	Harts-Pass	48.72000N / 120.66000W	1978	1980-2019
USC00453546	HATTON-9-SE	46.72250N / 118.65250W	459	1905-2019
USC00453730	HOLDEN-VILLAGE	48.19890N / 120.77360W	981	1962-2019
USW00094225	HOQUIAM-BOWERMAN-AP	46.97280N / 123.93030W	4	1953-2019
USC00453826	HUMPTULIPS-SALMON-HATCHERY	47.23360N / 123.98970W	43	1987-2019
USC00453883	ICE-HARBOR-DAM	46.24470N / 118.87860W	112	1957-2019
USS0022C09S	June-Lake	46.15000N / 122.15000W	1049	1980-2019
USC00454084	KALAMA-FALLS-HATCHERY	46.01640N / 122.73250W	95	1967-2019
USC00454154	KENNEWICK-HCN	46.21110N / 119.10110W	119	1894-2019
USC00454169	KENT	47.41720N / 122.24330W	9	1912-2019
USC00454338	LACROSSE	46.81670N / 117.88310W	450	1908-2019
USC00454446	LAKE-WENATCHEE	47.83750N / 120.79780W	624	1894-2008

ID	Name	Lat. / Lon.	Elv. (m)	Years
USC00454486	LANDSBURG	47.37670N / 121.96140W	163	1903-2019
USC00454572	LEAVENWORTH-3-S	47.55860N / 120.67500W	344	1914-2019
USC00454679	LIND-3-NE	47.00220N / 118.56580W	497	1931-2019
USS0021C26S	Lone-Pine	46.27000N / 121.96000W	1198	1978-2019
USC00454748	LONG-BEACH-EXP-STN-HCN	46.36750N / 124.03780W	8	1967-2018
USC00454764	LONGMIRE-RAINIER-NPS-HCN	46.74920N / 121.81200W	842	1978-2019
USC00454769	LONGVIEW-HCN	46.15060N / 122.91640W	4	1925-2019
USS0021C39S	Lost-Horse	46.36000N / 121.08000W	1561	1989-2019
USC00454841	LOWER-MONUMENTAL-DAM	46.56420N / 118.53970W	140	1962-2007
USS0020A23S	Lyman-Lake	48.20000N / 120.92000W	1823	1979-2019
USC00455086	MATLOCK-8-S	47.14560N / 123.40060W	34	1985-2019
USC00455110	MAYFIELD-PWR-PLT	46.50440N / 122.59390W	85	1980-2019
USC00455133	MAZAMA	48.60080N / 120.42750W	653	1950-2019
USC00455224	MCMILLIN-RSVR-HCN	47.13580N / 122.25580W	177	1941-2019
USC00455231	MCNARY-DAM	45.94060N / 119.29780W	110	1954-2007
USC00455305	MERWIN-DAM	45.95470N / 122.56390W	68	1971-2019
USC00455326	METHOW-2-S	48.10750N / 120.00780W	346	1970-2017
USC00455387	MILL-CREEK-DAM	46.07560N / 118.27420W	358	1948-2019
USC00455525	MONROE	47.84530N / 121.99440W	37	1929-2019
USS0021C17S	Morse-Lake	46.91000N / 121.48000W	1649	1978-2019
USW00024110	MOSES-LAKE-GRANT-CO-AP	47.20780N / 119.31920W	365	1949-2019
USS0021B21S	**MOUNT GARDNER**	**47.35000N / 121.56670W**	**890**	**2010-2017**
USS0023B06S	Mount-Crag	47.76000N / 123.03000W	1207	1989-2019
USC00455688	MOXEE-CITY-10-E	46.50530N / 120.16780W	472	1946-2018
USC00455659	MT-ADAMS-RS	45.99970N / 121.54030W	594	1909-2019
USC00455678	MT-VERNON-3-WNW	48.44030N / 122.38670W	4	1956-2005
USC00455704	MUD-MTN-DAM	47.14140N / 121.93560W	399	1939-2019
USC00455774	NASELLE-2-ENE	46.37250N / 123.75310W	15	1929-2019
USC00455840	NEWHALEM	48.67580N / 121.24190W	160	1959-2019
USC00455844	NEWPORT	48.18420N / 117.04750W	659	1909-2019
USC00455946	NORTHPORT-HCN	48.87420N / 117.86670W	450	1899-2019
USC00456039	ODESSA-HCN	47.33280N / 118.69670W	470	1902-2019
USS0021B55S	Olallie-Meadows	47.37000N / 121.44000W	1228	1980-2019
USC00456096	OLGA-2-SE-HCN	48.61170N / 122.80640W	24	1891-2016
USW00024227	OLYMPIA-AP-GSN-72792	46.97330N / 122.90330W	57	1941-2019
USC00456123	OMAK-4-N	48.46080N / 119.51670W	395	1909-2014
USC00456121	OMAK-72789	48.41670N / 119.53330W	259	1980-2015
USW00094197	OMAK-AP	48.46080N / 119.51670W	395	1998-2019
USC00456215	OTHELLO-6-ESE	46.78860N / 119.04610W	363	1941-2002
USC00456262	PACKWOOD	46.60920N / 121.67440W	323	1924-2019
USC00456295	PALMER-3-ESE	47.30580N / 121.85140W	280	1924-2019
USS0021C35S	Paradise	46.78000N / 121.75000W	1564	1980-2019
USS0020A12S	Park-Creek-Ridge	48.44000N / 120.92000W	1402	1978-2019
USW00024163	PASCO-TRI-CITIES-AP	46.26670N / 119.11670W	124	1945-2019
USS0021C33S	Pigtail-Peak	46.62000N / 121.39000W	1768	1980-2019
USC00456534	PLAIN	47.78500N / 120.64560W	590	1937-2019
USC00456610	POMEROY-HCN	46.46720N / 117.58830W	590	1891-2018
USS0020B24S	Pope-Ridge	47.99000N / 120.57000W	1094	1980-2019
USC00456624	PORT-ANGELES-HCN	48.11390N / 123.43170W	27	1933-2008

ID	Name	Lat. / Lon.	Elv. (m)	Years
USW00094266	PORT-ANGELES-INTL-AP	48.12030N / 123.49830W	88	1998-2019
USC00456678	PORT-TOWNSEND-HCN	48.11610N / 122.75860W	31	1891-2010
USS0021C14S	Potato-Hill	46.35000N / 121.51000W	1375	1981-2019
USC00456747	PRIEST-RAPIDS-DAM	46.64610N / 119.90610W	131	1956-2019
USC00456768	PROSSER	46.20140N / 119.75810W	253	1925-2019
USC00456789	PULLMAN-2-NW-HCN	46.76030N / 117.18610W	767	1940-2019
USW00094129	PULLMAN-MOSCOW-RGNL-AP	46.74390N / 117.10860W	778	1998-2019
USS0017B04S	Quartz-Peak	47.88000N / 117.09000W	1433	1986-2019
USC00456846	QUILCENE-2-SW	47.80920N / 122.91360W	38	1920-2019
USW00094240	QUILLAYUTE-STATE-AP-72797	47.93750N / 124.55500W	56	1966-2019
USC00456880	QUINCY	47.22360N / 119.85250W	392	1941-2019
USC00456896	RAINER-OHANAPECOSH	46.73220N / 121.57280W	594	1926-2019
USC00456898	RAINIER-PARADISE-RS	46.78580N / 121.74250W	1654	1916-2019
USS0020A09S	Rainy-Pass	48.52000N / 120.74000W	1491	1980-2019
USC00456909	RANDLE-1-E	46.53310N / 121.93280W	274	1924-2018
USC00456914	RAYMOND-2-S-HCN	46.65330N / 123.73000W	9	1980-2019
USW00094248	RENTON-MUNI-AP	47.49330N / 122.21440W	9	1998-2019
USC00456974	REPUBLIC	48.64690N / 118.73140W	799	1899-2019
USS0021B17S	**REX RIVER**	**47.30000N / 121.60000W**	**1161**	**1996-2018**
USC00457015	RICHLAND	46.31190N / 119.26330W	114	1944-2019
USC00457059	RITZVILLE-1-SSE-HCN	47.11750N / 118.37140W	568	1899-2019
USC00457180	ROSALIA	47.23250N / 117.36250W	733	1893-2019
USC00457185	ROSS-DAM	48.72720N / 121.07220W	377	1960-2019
USS0019A02S	Salmon-Meadows	48.66000N / 119.84000W	1359	1980-2019
USS0021B51S	Sasse-Ridge	47.38000N / 121.06000W	1323	1983-2019
USC00457342	SATUS-PASS-2-SSW	45.94810N / 120.66690W	788	1968-2019
USW00024234	SEATTLE-BOEING-FLD	47.53030N / 122.30080W	6	1948-2019
USW00094290	SEATTLE-SAND-PT-WSFO	47.68720N / 122.25530W	18	1986-2019
USW00024233	SEATTLE-TACOMA-INTL-AP-72793	47.44440N / 122.31390W	113	1948-2019
USC00457507	SEDRO-WOOLLEY-HCN	48.49580N / 122.23550W	18	1896-2019
USC00457544	SEQUIM-2-E	48.08500N / 123.06390W	15	1980-2019
USS0022C10S	Sheep-Canyon	46.19000N / 122.25000W	1216	1980-2019
USC00457584	SHELTON	47.20000N / 123.10000W	7	1931-1999
USW00094227	SHELTON-SANDERSON-FLD	47.23810N / 123.14080W	83	1998-2019
USC00457696	SKAMANIA-FISH-HATCHERY	45.62190N / 122.21780W	133	1965-2019
USS0021B60S	**SKOOKUM CREEK**	**47.68330N / 121.60000W**	**1009**	**1996-2017**
USC00457727	SMYRNA	46.83670N / 119.66330W	171	1951-2008
USC00457773	SNOQUALMIE-FALLS-HCN	47.54140N / 121.83610W	134	1898-2019
USS0017C06S	**SOURDOUGH GULCH**	**46.23330N / 117.38330W**	**1219**	**2002-2015**
USS0021C20S	Spencer-Meadow	46.18000N / 121.93000W	1036	1981-2019
USS0022C12S	Spirit-Lake	46.26000N / 122.18000W	1073	1984-2019
USW00094176	SPOKANE-FELTS-FLD	47.68310N / 117.32140W	595	1998-2019
USW00024157	SPOKANE-INTL-AP-HCN-72785	47.62170N / 117.52810W	717	1889-2019
USS0017C04S	**SPRUCE SPRINGS**	**46.16670N / 117.53330W**	**514**	**2004-2013**
USC00457267	ST.-JOHN-HCN	47.09330N / 117.58780W	595	1963-2019
USS0021B10S	Stampede-Pass	47.27000N / 121.34000W	1174	1980-2019
USW00024237	STAMPEDE-PASS	47.27670N / 121.33720W	1207	1944-2019
USC00458034	STARTUP-1-E	47.86640N / 121.71750W	52	1924-2019
USC00458059	STEHEKIN-4-NW-HCN	48.35080N / 120.72640W	383	1906-2019

ID	Name	Lat. / Lon.	Elv. (m)	Years
USS0021B01S	Stevens-Pass	47.75000N / 121.09000W	1204	1980-2019
USC00458207	SUNNYSIDE-HCN	46.32360N / 120.01030W	228	1894-2013
USS0021C13S	Surprise-Lakes	46.09000N / 121.76000W	1308	1978-2019
USC00458278	TACOMA-#1	47.24720N / 122.41220W	8	1982-2019
USW00094274	TACOMA-NARROWS-AP	47.26750N / 122.57610W	89	1999-2019
USW00024219	THE-DALLES-MUNI-AP	45.61940N / 121.16610W	72	1948-2019
USS0020A07S	Thunder-Basin	48.53000N / 120.99000W	1317	1987-2019
USW00024241	TOLEDO-FAA-AP	46.48330N / 122.81670W	116	1948-2007
USC00458508	TOLT-S-FK-RSVR	47.70000N / 121.69080W	610	1962-2019
USS0017C05S	Touchet	46.12000N / 117.85000W	1686	1980-2019
USS0020B25S	Trough	47.23000N / 120.29000W	1670	1978-2019
USC00458715	UPPER-BAKER-DAM	48.65250N / 121.69310W	210	1965-2019
USS0020B07S	Upper-Wheeler	47.29000N / 120.37000W	1320	1980-2019
USC00458773	VANCOUVER-4-NNE-HCN	45.67780N / 122.65110W	64	1856-2019
USW00094298	VANCOUVER-PEARSON-AP	45.62080N / 122.65720W	9	1998-2019
USW00024160	WALLA-WALLA-RGNL-AP-HCN	46.09470N / 118.28690W	355	1949-2019
USW00094103	WALLA-WALLA-WSO-CITY	46.03330N / 118.33330W	289	1994-1995
USC00458959	WAPATO	46.43530N / 120.42030W	256	1915-2013
USC00459012	WATERVILLE-HCN	47.64970N / 120.08000W	812	1893-2019
USC00459021	WAUNA-3-W	47.37250N / 122.70280W	5	1938-2015
USC00459058	WELLPINIT	47.89640N / 117.99330W	759	1923-2007
USS0021A31S	**WELLS CREEK**	**48.85000N / 121.78330W**	**1228**	**1996-2015**
USC00459079	WENATCHEE-EXP-STN	47.43330N / 120.35000W	244	1950-2013
USC00459074	WENATCHEE-HCN	47.42890N / 120.31000W	191	1931-2019
USW00094239	WENATCHEE-PANGBORN-AP	47.39780N / 120.20140W	375	1959-2019
USW00024255	WHIDBEY-ISLAND-NAS-69023	48.35000N / 122.66670W	14	1945-2019
USS0021C28S	White-Pass-E.S.	46.64000N / 121.38000W	1353	1980-2019
USC00459200	WHITMAN-MISSION	46.04360N / 118.46280W	193	1962-2019
USC00459238	WILBUR-HCN	47.76810N / 118.72390W	690	1892-2019
USC00459376	WINTHROP-1-WSW-HCN	48.47420N / 120.18860W	533	1906-2019
USW00024243	YAKIMA-AIR-TERMINAL-72781	46.56830N / 120.54280W	324	1946-2019

Table A3. Snowpack Telemetry (SNOTEL) stations used in the WRF model evaluation.

ID	Name	Lat./Lon.	Elv. (m)	Years
908	Alpine Meadows	47.78000N / 121.70000W	1067	1994-2018
990	Beaver Pass	48.88000N / 121.26000W	1106	2001-2018
352	Blewett Pass	47.35000N / 120.68000W	1292	1980-2018
1080	Brown Top	48.93000N / 121.20000W	1777	2009-2018
1107	Buckinghorse	47.71000N / 123.46000W	1484	2008-2018
375	Bumping Ridge	46.81000N / 121.33000W	1405	1978-2018
376	Bunchgrass Mdw	48.69000N / 117.18000W	1524	1980-2018
942	Burnt Mountain	47.04000N / 121.94000W	1271	1999-2018
1109	Calamity	45.90000N / 122.22000W	762	2008-2018
1085	Cayuse Pass	46.87000N / 121.53000W	1597	2006-2018
418	Corral Pass	47.02000N / 121.46000W	1768	1980-2018
420	Cougar Mountain	47.28000N / 121.67000W	975	1980-2018
943	Dungeness	47.87000N / 123.08000W	1222	1998-2018
998	Easy Pass	48.86000N / 121.44000W	1606	2008-2018
910	Elbow Lake	48.69000N / 121.91000W	927	1995-2018
478	Fish Lake	47.54000N / 121.09000W	1045	1983-2018
1159	Gold Axe Camp	48.95000N / 118.99000W	1634	2010-2018
1256	Gold Mountain	48.19000N / 118.46000W	1338	2014-2018
502	Green Lake	46.55000N / 121.17000W	1804	1982-2018
507	Grouse Camp	47.28000N / 120.49000W	1643	1980-2018
515	Harts Pass	48.72000N / 120.66000W	1978	1980-2018
928	Huckleberry Creek	47.07000N / 121.59000W	686	1997-2018
1129	Indian Rock	45.99000N / 120.81000W	1634	2008-2018
553	June Lake	46.15000N / 122.15000W	1049	1980-2018
591	Lone Pine	46.27000N / 121.96000W	1198	1978-2018
599	Lost Horse	46.36000N / 121.08000W	1561	1989-2018
606	Lyman Lake	48.20000N / 120.92000W	1823	1979-2018
1069	Lynn Lake	47.20000N / 121.78000W	1189	2007-2018
999	Marten Ridge	48.76000N / 121.70000W	1073	2006-2018
897	Meadows Pass	47.28000N / 121.47000W	985	1993-2018
1011	MF Nooksack	48.82000N / 121.93000W	1515	2002-2018
642	Morse Lake	46.91000N / 121.48000W	1649	1978-2018
644	Moses Mtn	48.36000N / 119.08000W	1527	1991-2018
648	Mount Crag	47.76000N / 123.03000W	1207	1989-2018
898	Mount Gardner	47.36000N / 121.57000W	890	1993-2018
941	Mowich	46.93000N / 121.95000W	963	1998-2018
1259	Muckamuck	48.59000N / 119.87000W	1362	2014-2018
672	Olallie Meadows	47.37000N / 121.44000W	1228	1980-2018
679	Paradise	46.78000N / 121.75000W	1564	1980-2018
681	Park Creek Ridge	48.44000N / 120.92000W	1402	1978-2018
1104	Pepper Creek	46.10000N / 121.96000W	652	2007-2018
692	Pigtail Peak	46.62000N / 121.39000W	1768	1981-2018
1263	Pinto Rock	46.32000N / 121.94000W	1353	2014-2018
699	Pope Ridge	47.99000N / 120.57000W	1094	1981-2018
702	Potato Hill	46.35000N / 121.51000W	1375	1981-2018
707	Quartz Peak	47.88000N / 117.09000W	1433	1986-2018
711	Rainy Pass	48.52000N / 120.74000W	1490	1980-2018
911	Rex River	47.30000N / 121.60000W	1161	1995-2018

ID	Name	Lat./Lon.	Elv. (m)	Years
728	Salmon Meadows	48.66000N / 119.84000W	1359	1980-2018
734	Sasse Ridge	47.38000N / 121.06000W	1323	1983-2018
1231	Satus Pass	45.99000N / 120.68000W	1207	2012-2018
1068	Sawmill Ridge	47.16000N / 121.42000W	1414	2006-2018
1043	Sentinel Butte	48.86000N / 118.40000W	1426	2003-2018
748	Sheep Canyon	46.19000N / 122.25000W	1216	1980-2018
1257	Skate Creek	46.64000N / 121.83000W	1149	2014-2018
912	Skookum Creek	47.68000N / 121.61000W	1009	1995-2018
985	Sourdough Gulch	46.24000N / 117.39000W	1219	2000-2018
776	Spencer Meadow	46.18000N / 121.93000W	1036	1981-2018
777	Spirit Lake	46.26000N / 122.18000W	1073	1984-2018
984	Spruce Springs	46.18000N / 117.54000W	1737	2000-2018
788	Stampede Pass	47.27000N / 121.34000W	1173	1982-2018
791	Stevens Pass	47.75000N / 121.09000W	1204	1980-2018
804	Surprise Lakes	46.09000N / 121.76000W	1308	1978-2018
975	Swamp Creek	48.57000N / 120.78000W	1198	1999-2018
1012	Swift Creek	46.16000N / 122.18000W	1353	2002-2018
817	Thunder Basin	48.53000N / 120.99000W	1317	1987-2018
899	Tinkham Creek	47.33000N / 121.47000W	911	1993-2018
824	Touchet	46.12000N / 117.85000W	1686	1980-2018
1171	Trinity	48.07000N / 120.85000W	893	2010-2018
832	Trough	47.23000N / 120.29000W	1670	1978-2018
841	Upper Wheeler	47.29000N / 120.37000W	1320	1980-2018
974	Waterhole	47.94000N / 123.43000W	1527	1999-2018
909	Wells Creek	48.87000N / 121.79000W	1228	1995-2018
863	White Pass E.S.	46.64000N / 121.38000W	1353	1980-2018

Appendix B: Maps Comparing WRF-GCM and Observations

Comparisons between the raw (not bias-corrected) WRF projections and weather station observations.

Figure B1. Maps of the annual average daily minimum temperature biases for WRF-GCM simulations (1970-2015). One map is shown for each GCM. The size of each circle denotes the bias, while the color denotes the sign of the bias.

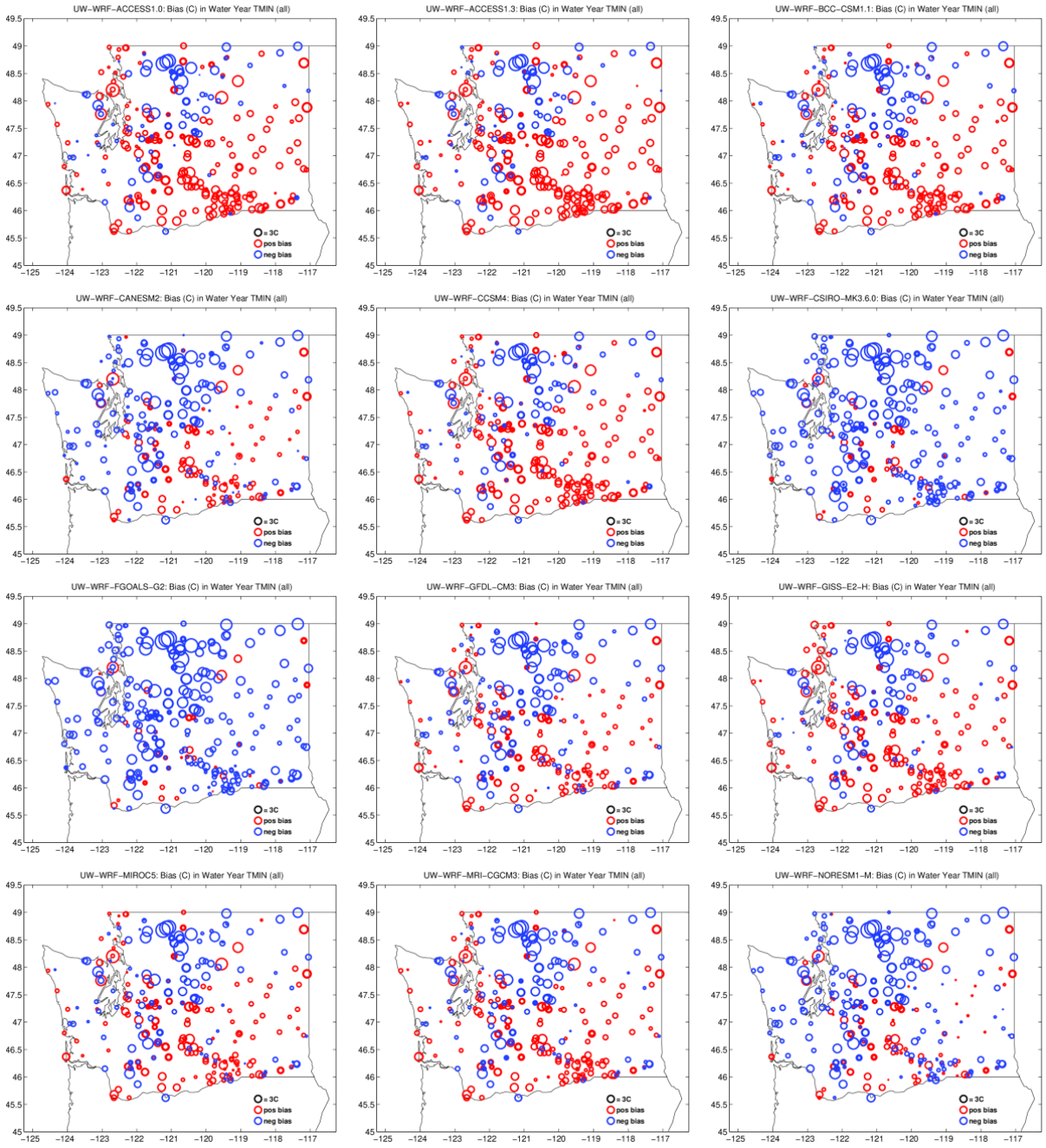

Figure B2. As in Figure B1 except showing maps of the annual average daily maximum temperature biases.

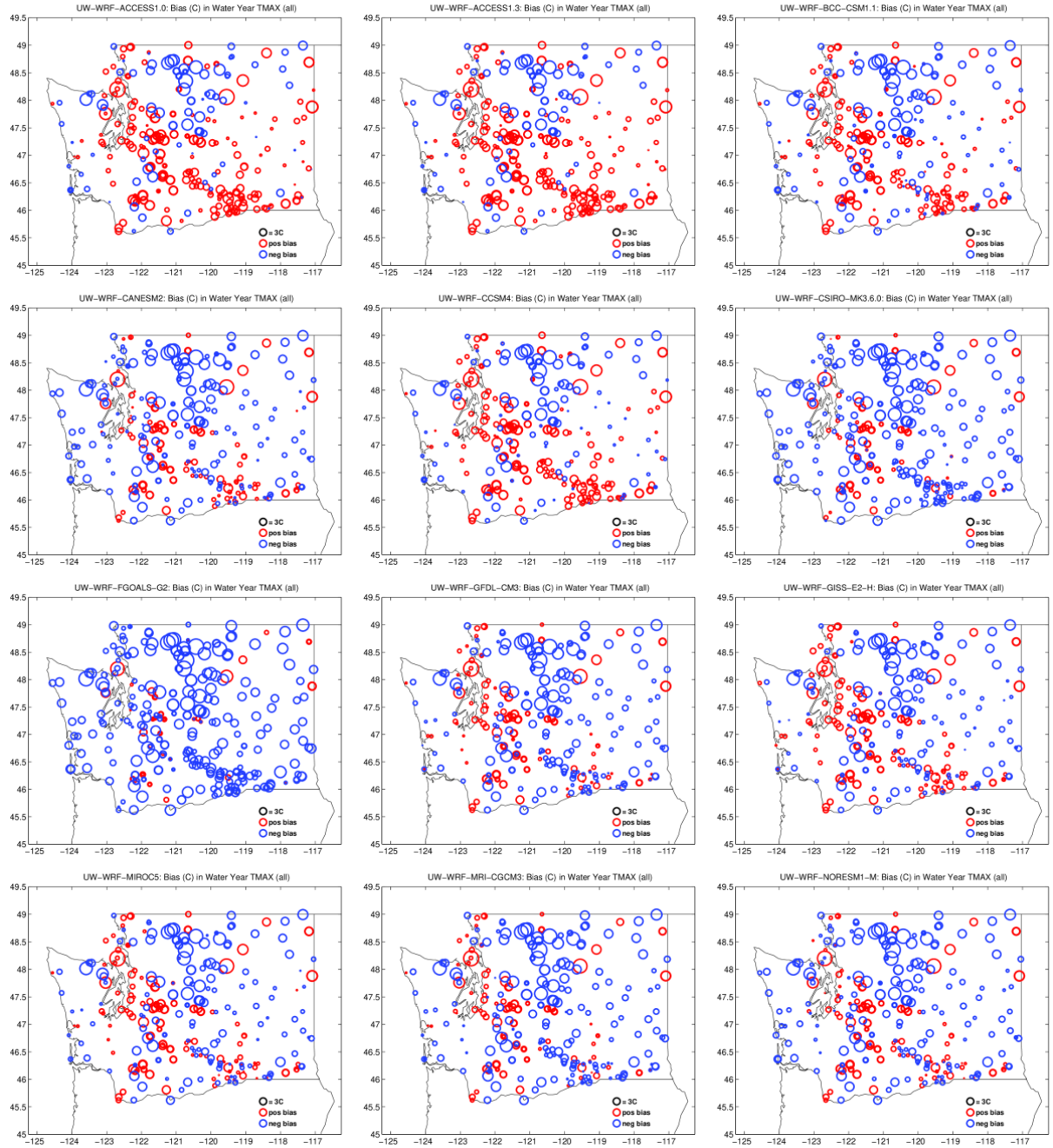

Figure B3. As in Figure B1 except showing maps of the annual average daily total precipitation biases.

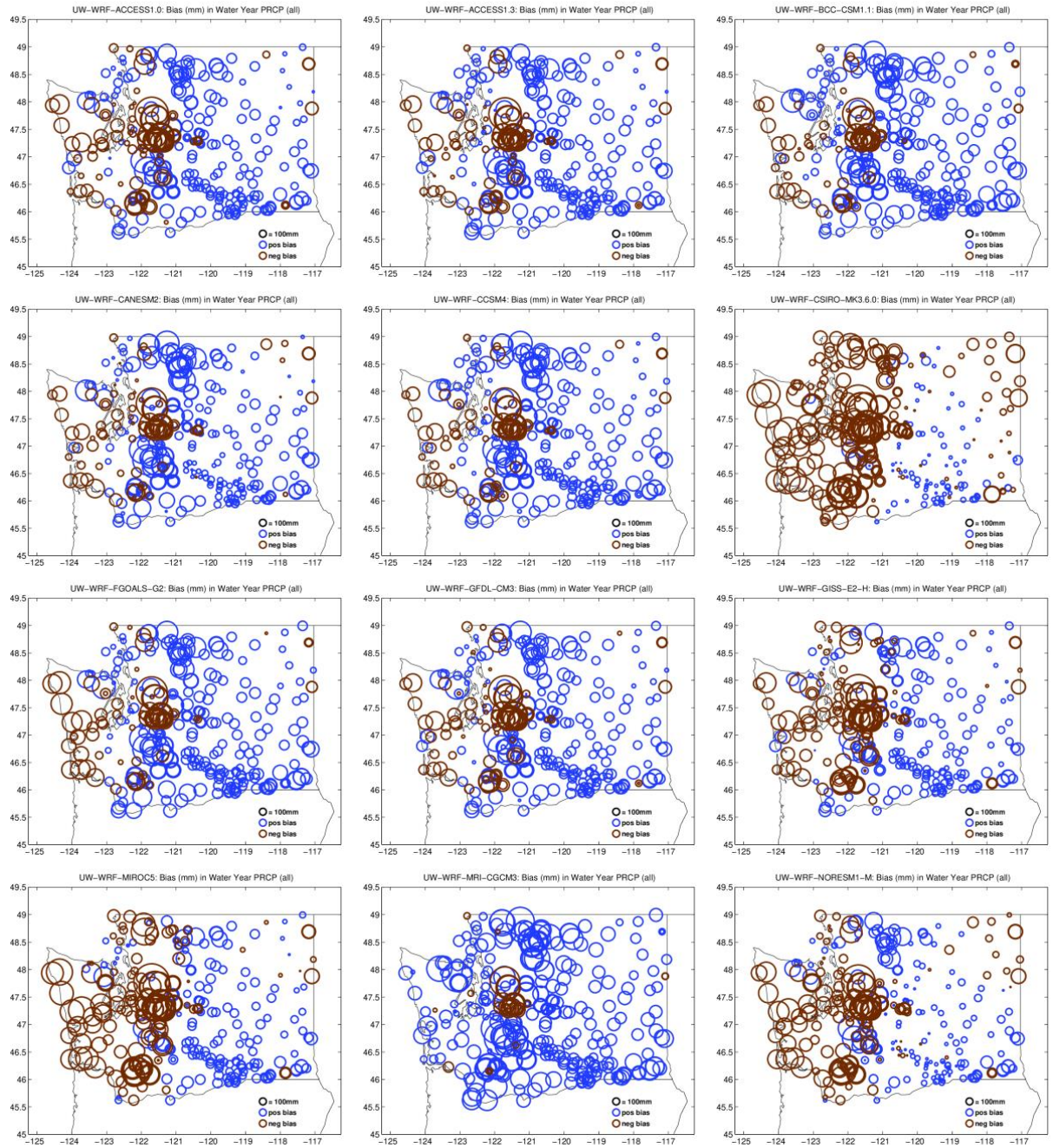

Appendix C: Streamflow Gauges used in VIC Evaluation

Table C1: USGS streamflow gauges used to evaluate VIC model results.

ID	Name	Lat.	Lon.	Area (km^2)
13334450	ASOTIN CR BLW CONFLUENCE NR ASOTIN	46.27361	-117.29139	270
13335050	ASOTIN CR AT ASOTIN	46.34072	-117.05599	841
13334700	ASOTIN CR BLW KEARNEY GULCH NR ASOTINSH.	46.32627	-117.15266	441
14017000	TOUCHET R AT BOLLES	46.27431	-118.22190	942
14113000	KLICKITAT R NR PITT	45.75651	-121.21007	3366
14123500	WHITE SALMON R NR UNDERWOOD	45.75206	-121.52702	1000
12510500	YAKIMA R AT KIONA	46.25347	-119.47808	14536
14111400	KLICKITAT R BL SUMMIT CR NR GLENWOOD	45.96234	-121.10229	1967
13344500	TUCANNON R NR STARBUCK	46.50542	-118.06634	1117
12508990	YAKIMA R AT MABTON	46.23124	-119.99949	13858
14212000	SALMON CR NR BATTLE GROUND	45.77373	-122.44565	47
14222500	EAST FORK LEWIS R NR HEISSON	45.83678	-122.46621	324
14219000	CANYON CR NR AMBOY	45.93983	-122.31704	167
14216000	LEWIS R ABOVE MUDDY R NR COUGAR	46.06039	-121.98453	595
14220500	LEWIS R AT ARIEL	45.95178	-122.56399	1898
14216500	MUDDY CR BLW CLEAR CR NR COUGAR	46.07567	-121.99870	350
14219800	SPEELYAI CR NR COUGAR	46.00761	-122.34732	33
12513000	ESQUATZEL COULEE AT CONNELL	46.66347	-118.86333	602
14107000	KLICKITAT R ABOVE WEST FORK NR GLENWOOD	46.26484	-121.24507	394
12512550	PROVIDENCE COULEE NR CUNNINGHAM	46.80292	-118.81639	138
12500450	YAKIMA R ABOVE AHTANUM CR AT UNION GAP	46.53429	-120.46729	9018
12502500	AHTANUM CR AT UNION GAP	46.53596	-120.47340	446
14232500	CISPUS R NR RANDLESH.	46.44706	-121.86398	825
14243000	COWLITZ R AT CASTLE ROCK	46.27483	-122.91456	5774
14241500	SOUTH FORK TOUTLE R AT TOUTLE	46.32205	-122.69706	310
14240525	NF TOUTLE R BLW SRS NR KID VALLEY	46.37177	-122.57900	379
14233500	COWLITZ R NR KOSMOS	46.46622	-122.10899	2653
14233400	COWLITZ R NR RANDLE	46.47011	-122.09871	2651
14242580	TOUTLE R AT TOWER ROAD NR SILVER LAKE	46.33372	-122.84011	1292
14231000	COWLITZ R AT RANDLE	46.53233	-121.95676	1378
14226500	COWLITZ R AT PACKWOOD	46.61289	-121.67925	731
12484500	YAKIMA R AT UMTANUM	46.86263	-120.48007	4139
14238000	COWLITZ R BLW MAYFIELD DAM	46.51038	-122.61622	3594
12464770	CRAB CR AT ROCKY FORD ROAD NR RITZVILLE	47.30265	-118.36914	1182
12020800	SOUTH FORK CHEHALIS R NR WILDWOOD	46.44483	-123.08374	70
14236200	TILTON R AB BEAR CANYON CR NR CINEBAR	46.59538	-122.45956	361
12467000	CRAB CR NR MOSES LAKE	47.18931	-119.26586	5348
12024000	SOUTH FORK NEWAUKUM R NR ONALASKA	46.57566	-122.68512	109
12010000	NASELLE R NR NASELLE	46.37399	-123.74348	142
12464800	COAL CR AT MOHLER	47.40682	-118.31887	159
12082500	NISQUALLY R NR NATIONAL	46.75261	-122.08372	350
12083000	MINERAL CR NR MINERAL	46.74427	-122.14455	199
12465000	CRAB CR AT IRBY	47.36042	-118.85000	2707
12025000	NEWAUKUM R NR CHEHALIS	46.62010	-122.94513	405
12488500	AMERICAN R NR NILE	46.97762	-121.16870	205

ID	Name	Lat.	Lon.	Area (km²)
12024400	NF NEWAUKUM R ABOVE BEAR CR NR FOREST	46.66733	-122.77012	77
12470500	ROCKY FORD CR NR EPHRATA	47.31264	-119.44559	1089
12020000	CHEHALIS R NR DOTY	46.61732	-123.27764	294
12025700	SKOOKUMCHUCK R NR VAIL	46.77260	-122.59401	103
12086500	NISQUALLY R AT LA GRANDE	46.84344	-122.33067	760
12092000	PUYALLUP R NR ELECTRON	46.90372	-122.03511	241
12087000	MASHEL R NR LA GRANDE	46.85677	-122.30261	214
12026150	SKOOKUMCHUCK R BL BLDY RUN CR NR CENTRALIA	46.79010	-122.73540	170
12088000	OHOP CR NR EATONVILLE	46.88094	-122.27900	89
12026400	SKOOKUMCHUCK R NR BUCODA	46.77205	-122.92430	299
12027500	CHEHALIS R NR GRAND MOUND	46.77593	-123.03569	2327
12013500	WILLAPA R NR WILLAPA	46.65093	-123.65266	338
12079000	DESCHUTES R NR RAINIER	46.85204	-122.66873	224
12479500	YAKIMA R AT CLE ELUM	47.19123	-120.94703	1299
12094000	CARBON R NR FAIRFAX	47.02788	-122.03261	205
12089500	NISQUALLY R AT MCKENNA	46.93343	-122.56096	1366
12093500	PUYALLUP R NR ORTING	47.03927	-122.20789	438
12097500	GREENWATER R AT GREENWATER	47.15344	-121.63565	190
12465400	WILSON CR BLW CORBETT DRAW NR ALMIRA	47.66293	-118.93057	870
12097850	WHITE R BLW CLEARWATER R NR BUCKLEY	47.14677	-121.86011	970
12104500	GREEN R NR LESTERSH.	47.20761	-121.55315	249
12433200	CHAMOKANE CR BLW FALLS NR LONG LAKE	47.86155	-117.85885	469
12098500	WHITE R NR BUCKLEY	47.15121	-121.94983	1040
12095000	SOUTH PRAIRIE CR AT SOUTH PRAIRIE	47.13955	-122.09261	206
12099200	WHITE R ABOVE BOISE CR AT BUCKLEY	47.17389	-122.00806	1062
12100000	WHITE R AT BUCKLEY	47.17427	-122.02039	1105
12017000	NORTH R NR RAYMOND	46.80732	-123.85072	569
12099600	BOISE CR AT BUCKLEY	47.17594	-122.01844	42
12080010	DESCHUTES R AT E ST BRIDGE AT TUMWATER	47.01176	-122.90319	402
12031000	CHEHALIS R AT PORTER	46.93926	-123.31432	3361
12462500	WENATCHEE R AT MONITOR	47.49929	-120.42452	3372
12090400	NORTH FORK CLOVER CR NR PARKLAND	47.13454	-122.41512	15
12096500	PUYALLUP R AT ALDERTON	47.18510	-122.22956	1143
12081000	WOODLAND CR NR OLYMPIA	47.07149	-122.81736	64
12105900	GREEN R BLW HOWARD A HANSON DAM	47.28371	-121.79788	574
12090500	CLOVER CR NR TILLICUM	47.14593	-122.51040	164
12114500	CEDAR R BLW BEAR CR NR CEDAR FALLS	47.34205	-121.54899	67
12102190	SWAN CR AT 80TH ST EAST NR TACOMA	47.18454	-122.39373	6
12105710	NORTH FORK GREEN R NR LEMOLO	47.30566	-121.77344	66
12035002	CHEHALIS R NR SATSOP	46.97204	-123.49155	4562
12101500	PUYALLUP R AT PUYALLUP	47.20843	-122.32707	2449
12106700	GREEN R AT PURIFICATION PLANT NR PALMER	47.30510	-121.85067	598
12115500	REX R NR CEDAR FALLS	47.35066	-121.66316	35
12108500	NEWAUKUM CR NR BLACK DIAMOND	47.27566	-122.05956	71
12091100	FLETT CR AT TACOMA	47.18954	-122.52012	35
12115000	CEDAR R NR CEDAR FALLS	47.37011	-121.62510	103
12035000	SATSOP R NR SATSOP	47.00065	-123.49488	770
12091290	LEACH CR AT MEADOW PARK GC AT UNIVERSITY PLACE	47.19843	-122.52096	17
12091300	LEACH CR NR STEILACOOM	47.19815	-122.52263	13

ID	Name	Lat.	Lon.	Area (km²)
12458000	ICICLE CR ABV SNOW CR NR LEAVENWORTHSH.	47.54095	-120.72009	499
12091500	CHAMBERS CR BL LEACH CR NR STEILACOOM	47.19760	-122.52874	258
12115700	BOULDER CR NR CEDAR FALLS	47.36622	-121.69288	13
12100496	WHITE R NR AUBURN	47.26593	-122.22984	1231
12091200	LEACH CR NR FIRCREST	47.22149	-122.50929	12
12459000	WENATCHEE R AT PESHASTIN	47.58318	-120.61953	2588
12143400	SF SNOQUALMIE R AB ALICE CR NR GARCIA	47.41511	-121.58732	108
12452990	ENTIAT R NR ENTIAT	47.66318	-120.25063	1075
12037400	WYNOOCHEE R ABOVE BLACK CR NR MONTESANO	47.01148	-123.65544	400
12112600	BIG SOOS CR ABOVE HATCHERY NR AUBURN	47.31232	-122.16540	173
12113000	GREEN R NR AUBURN	47.31232	-122.20401	1067
12117000	TAYLOR CR NR SELLECK	47.38649	-121.84622	45
12117600	CEDAR R BLW DIVERSION NR LANDSBURG	47.37955	-121.98345	346
12116400	CEDAR R AT POWERPLANT AT CEDAR FALLS	47.41871	-121.78150	219
12116500	CEDAR R AT CEDAR FALLS	47.41705	-121.79205	220
12118500	ROCK CR NR MAPLE VALLEY	47.37982	-122.01734	33
12117500	CEDAR R NR LANDSBURG	47.39371	-121.95456	337
12143700	BOXLEY CR NR CEDAR FALLS	47.43260	-121.75233	3
12143900	BOXLEY CR NR EDGEWICK	47.44871	-121.73177	14
12143600	SF SNOQUALMIE R AT EDGEWICK	47.45260	-121.71788	165
12141300	MIDDLE FORK SNOQUALMIE R NR TANNER	47.48594	-121.64788	402
12113347	MILL CR AT EARTHWORKS PARK AT KENT	47.38316	-122.22484	7
12076800	GOLDSBOROUGH CR ABOVE 7TH STREET AT SHELTON	47.21176	-123.11293	155
12452890	MAD R AT ARDENVOIR	47.73679	-120.36870	236
12144000	SF SNOQUALMIE R AT NORTH BEND	47.49288	-121.79011	210
12120600	ISSAQUAH CR NR HOBART	47.45732	-122.00512	47
12452500	CHELAN R AT CHELAN	47.83458	-120.01313	2415
12113349	MILL CR NR MOUTH AT ORILLIA	47.43010	-122.24318	14
12434590	SANPOIL R ABOVE JACK CR AT KELLER	48.08432	-118.69140	2168
12457000	WENATCHEE R AT PLAINSH.	47.76290	-120.66620	1545
12144500	SNOQUALMIE R NR SNOQUALMIE	47.54510	-121.84234	977
12119000	CEDAR R AT RENTON	47.48260	-122.20346	448
12145500	RAGING R NR FALL CITY	47.53982	-121.90900	79
12452800	ENTIAT R NR ARDENVOIR	47.81846	-120.42314	526
12073500	HUGE CR NR WAUNA	47.38926	-122.69902	16
12142000	NF SNOQUALMIE R NR SNOQUALMIE FALLS	47.61483	-121.71344	166
12121600	ISSAQUAH CR NR MOUTH NR ISSAQUAH	47.55232	-122.04790	148
12059500	NORTH FORK SKOKOMISH R NR POTLATCH	47.32981	-123.24321	302
12456500	CHIWAWA R NR PLAIN	47.83735	-120.66232	446
12060500	SOUTH FORK SKOKOMISH R NR UNION	47.34037	-123.28016	198
12039005	HUMPTULIPS R BLW HWY 101 NR HUMPTULIPS	47.23148	-123.97406	344
12036000	WYNOOCHEE R ABOVE SAVE CR NR ABERDEEN	47.29898	-123.65322	191
12147600	SOUTH FORK TOLT R NR INDEX	47.70677	-121.60011	14
12058790	NF SKOKOMISH R NR LWR CUSHMAN DAM NR POTLATCH	47.39731	-123.20210	254
12148000	SOUTH FORK TOLT R NR CARNATION	47.68927	-121.71345	52
12120000	MERCER CR NR BELLEVUE	47.60288	-122.18096	37
12149000	SNOQUALMIE R NR CARNATION	47.66593	-121.92540	1561
12148300	SF TOLT R BL REGULATING BASIN NR CARNATION	47.69677	-121.78734	77
12148500	TOLT R NR CARNATION	47.69566	-121.82401	210

ID	Name	Lat.	Lon.	Area (km²)
12147500	NORTH FORK TOLT R NR CARNATION	47.71232	-121.78873	103
12124000	EVANS CR (ABOVE MOUTH) NR REDMOND	47.67510	-122.08123	34
12035450	BIG CR NR GRISDALE	47.37426	-123.63684	25
12035400	WYNOOCHEE R NR GRISDALE	47.38037	-123.60989	106
12449950	METHOW R NR PATEROS	48.07736	-119.98507	4645
12125200	SAMMAMISH R NR WOODINVILLE	47.70399	-122.14262	405
12120500	JUANITA CR NR KIRKLAND	47.70732	-122.21540	17
12128000	THORNTON CR NR SEATTLE	47.69565	-122.27624	31
12134500	SKYKOMISH R NR GOLD BAR	47.83732	-121.66678	1386
12056500	NF SKOKOMISH R BL STAIRCASE RPDS NR HOODSPORT	47.51426	-123.32989	147
12069550	BIG BEEF CR NR SEABECK	47.64065	-122.78515	33
12127100	SWAMP CR AT KENMORE	47.75593	-122.23374	59
12135000	WALLACE R AT GOLD BAR	47.86399	-121.68262	50
12039500	QUINAULT R AT QUINAULT LAKE	47.45759	-123.88935	688
12150800	SNOHOMISH R NR MONROE	47.83093	-122.04846	3979
12408500	MILL CR NR COLVILLE	48.57879	-117.86665	214
12138160	SULTAN R BLW POWERPLANT NR SULTAN	47.90732	-121.81540	244
12137290	SOUTH FORK SULTAN R NR SULTAN	47.94733	-121.62678	30
12070000	DOGFISH CR NR POUSLBO	47.75287	-122.64459	13
12054000	DUCKABUSH R NR BRINNON	47.68398	-123.01155	172
12409000	COLVILLE R AT KETTLE FALLS	48.59435	-118.06249	2602
12039300	NORTH FORK QUINAULT R NR AMANDA PARK	47.59592	-123.62434	190
12137800	SULTAN R BLW DIVERSION DAM NR SULTAN	47.95927	-121.79735	198
12155300	PILCHUCK R NR SNOHOMISH	47.93482	-122.07318	333
12052210	BIG QUILCENE R BLW DIVERSION NR QUILCENE	47.78454	-122.97961	129
12040500	QUEETS R NR CLEARWATER	47.53786	-124.31575	1153
12449500	METHOW R AT TWISP	48.36514	-120.11619	3425
12448998	TWISP R NR TWISP	48.36987	-120.14869	633
12397100	OUTLET CR NR METALINE FALLS	48.84492	-117.28774	135
12396900	SULLIVAN CR AB OUTLET CR NR METALINE FALLS	48.84631	-117.28691	181
12398000	SULLIVAN CR AT METALINE FALLS	48.86020	-117.36413	370
12186000	SAUK R AB WHITECHUCK R NR DARRINGTON	48.16872	-121.47067	398
12451000	STEHEKIN R AT STEHEKIN	48.32958	-120.69177	831
12157250	MISSION CR NR TULALIP	48.05843	-122.26736	21
12158040	TULALIP CR NR TULALIP	48.06843	-122.28792	41
12448500	METHOW R AT WINTHROP	48.47348	-120.17731	2684
12448000	CHEWUCH R AT WINTHROP	48.47709	-120.18647	1358
12158010	TULALIP CR ABOVE EAST BRANCH NR TULALIP	48.09926	-122.29098	25
12181100	SF CASCADE R AT S CASCADE GL NR MARBLEMOUNT	48.37012	-121.07428	7
12181200	SALIX CR AT S CASCADE GL NR MARBLEMOUNT	48.37096	-121.07761	0
12048000	DUNGENESS R NR SEQUIM	48.01426	-123.13268	405
12041200	HOH R AT US HIGHWAY 101 NR FORKS	47.80675	-124.25103	656
12167000	NF STILLAGUAMISH R NR ARLINGTON	48.26149	-122.04764	684
12447383	METHOW R ABOVE GOAT CR NR MAZAMA	48.57375	-120.38509	951
12044900	ELWHA R ABOVE LAKE MILLS NR PORT ANGELES	47.97009	-123.59074	513
12168500	PILCHUCK CR NR BRYANT	48.26593	-122.16403	136
12189500	SAUK R NR SAUK	48.42456	-121.56846	1855
12045500	ELWHA R AT MCDONALD BR NR PORT ANGELES	48.05481	-123.58325	695
12182500	CASCADE R AT MARBLEMOUNT	48.52623	-121.41541	444

ID	Name	Lat.	Lon.	Area (km^2)
12043000	CALAWAH R NR FORKS	47.96008	-124.39299	337
12439300	TONASKET CR AT OROVILLE	48.94294	-119.41367	157
12447390	ANDREWS CR NR MAZAMA	48.82292	-120.14592	58
12193500	BAKER R AT CONCRETE	48.53984	-121.74320	772
12179900	BACON CR BLW OAKES CR NR MARBLEMOUNT	48.60457	-121.39957	128
12175500	THUNDER CR NR NEWHALEM	48.67263	-121.07290	274
12178100	NEWHALEM CR NR NEWHALEM	48.65596	-121.23846	70
12201500	SAMISH R NR BURLINGTON	48.54594	-122.33822	224
12209000	SF NOOKSACK R NR WICKERSHAM	48.66428	-122.13349	268
12209490	SKOOKUM CR ABOVE DIVERSION NR WICKERSHAM	48.67150	-122.13960	58
12210000	SF NOOKSACK R AT SAXON BRIDGE	48.67761	-122.16654	332
12043300	HOKO R NR SEKIU	48.24146	-124.38383	135
12201960	BRANNIAN CR AT S BAY DR NR WICKERSHAM	48.66900	-122.28016	9
12201950	ANDERSON CR NR BELLINGHAM	48.67372	-122.26738	11
12207750	WARM CR NR WELCOME	48.76734	-121.96460	11
12207850	CLEARWATER CR NR WELCOME	48.78845	-122.02293	49
12208000	MF NOOKSACK R NR DEMING	48.77928	-122.10654	193
12202300	OLSEN CR NR BELLINGHAM	48.75122	-122.35350	10
12202310	CARPENTER CR NR BELLINGHAM	48.75400	-122.35405	3
12202420	MILL CR NR BELLINGHAM	48.75511	-122.41656	3
12210500	NOOKSACK R AT DEMING	48.81039	-122.20488	1501
12205000	NF NOOKSACK R BL CASCADE CR NR GLACIER	48.90596	-121.84431	272
12210900	ANDERSON CR AT SMITH ROAD NR GOSHEN	48.83261	-122.33905	26
12210700	NOOKSACK R AT NORTH CEDARVILLE	48.84178	-122.29433	1525
12206900	RACEHORSE CR AT NORTH FORK ROAD NR KENDALL	48.88484	-122.13321	27
12213100	NOOKSACK R AT FERNDALE	48.84483	-122.58934	1904

Appendix D: Instructions for Accessing the Tool

Before you can use WDFW's Culverts and Climate Change internet site, you must have a Secure Access Washington (SAW) account. Here's how to get one:

1. Go to the SAW home page: https://secureaccess.wa.gov/myAccess/saw/select.do

2. Click on the "SIGN UP!" button. On the next page enter: first name, last name, e-mail address, user name, and password. Remember your user name and password.

3. Play the "I am not a robot" game, and then hit "Submit." SAW will send an authentication message to your e-mail.

4. Click on the link in that e-mail. That takes you back to the SAW home page.

5. Click on the LOGIN button. You're done. You have a SAW account.

To use the Culverts and Climate Change internet site:

1. Begin by directing your internet browser to the Culverts and Climate Change internet site at https://culverts.wdfw-fish.us/. You will be taken to a page with a log in message.

2. Click on the "Log in" button and you will be directed to another page with a list of security systems.

3. Click on "Secure Access Washington" at the top of the list. You will be directed to the SAW home page.

4. Log in. You will be taken to a page that says "Hi guest!"

5. Click on the "Allow" button. Now you should be on the Culverts and Climate Change internet site.

Note: The first time you click on the "Generate Report" button, a bar with "Allow once" and "Options for this site" may appear. Click on either. If you click on "Options for this site", then select "Always allow" if you don't want to click to approve every time.

Appendix E: Applications/Outreach

This work is intended to directly support managers by providing information that can be used to design climate-adapted culverts. Our primary engagement has been with the Washington Department of Fish and Wildlife (WDFW), which is the state permitting authority for culverts, in particular the staff members that are co-authors on this work. The primary goal of this work is to provide improved projections of future flows and deliver them in an updated tool to facilitate their use in culvert design (the tool can be accessed here: https://wdfw.wa.gov/species-habitats/habitat-recovery/fish-passage/climate-change).

We also engaged directly with potential users of our new dataset and internet tool. We hosted a half-day workshop on October 11, 2019 in Olympia, Washington. The workshop was attended by 17 people from county governments, other state agencies, a public utility, and private consulting firms in Washington State; all of them interested in climate-adapted culverts. We explained the internet site and the science supporting it, gave a demonstration, and asked them to complete a hands-on exercise using the tool. The workshop ended with their impressions and ideas to make the internet site more useful and user-friendly (Table 7).

In addition to WDFW, we have also engaged with the Washington Department of Natural Resources (DNR). Since many of their culverts do not require fish passage, they are typically designed to withstand the 100-year peak flow event. We provided DNR staff with our projections for use in evaluating their design standards across the state, and presented to their team to support interpretation and use of the new projections.

Although our primary focus has been Washington State, this work has applicability for any agency or practitioner wishing to evaluate culvert designs. Although we made contact with several agencies working in Oregon and Idaho, our primary engagement beyond Washington State was with the National Marine Fisheries Service (NMFS). Jean Castillo, at NMFS, asked us to review their draft guidance on incorporating climate change in the design of fish passage facilities (NMFS, 2022).